

Article

Studying the Relationship between the Traffic Flow Structure, the Traffic Capacity of Intersections, and Vehicle-Related Emissions

Vladimir Shepelev ^{1,*} , Aleksandr Glushkov ², Ivan Slobodin ¹ and Mohammed Balfaqih ³ 

¹ Department of Automobile Transportation, South Ural State University (National Research University), 454080 Chelyabinsk, Russia

² Department of Mathematical and Computer Modeling, South Ural State University (National Research University), 454080 Chelyabinsk, Russia; glushkovai@susu.ru

³ Department of Computer and Network Engineering, College of Computer Science and Engineering, University of Jeddah, Jeddah 23890, Saudi Arabia; mabalfaqih@uj.edu.sa

* Correspondence: shepelevvd@susu.ru

Abstract: This paper proposes a new approach to assessing the impact of changes in the traffic flow on pollutant emissions and the traffic capacity of signal-controlled intersections. We present an intelligent vision system tailored to monitor the traffic behavior at signal-controlled intersections in urban areas. Traffic cameras are used to collect real-time vehicle traffic data. Our system provides valuable insight into the relationship between traffic flows, emissions, and intersection capacity. This study shows how changes in the traffic composition reduce the traffic capacity of intersections and increase emissions, especially those involving fine dust particles. Using the combination of fuzzy logic methods and Gaussian spline distribution functions, we demonstrate the variability of these relationships and highlight the need to further study compromises between mobility and air quality. Ultimately, our results offer promising opportunities for the development of intelligent traffic management systems aimed at balancing the demands of urban mobility while minimizing environmental impact. This study demonstrates the importance of taking into account the correlation between the change in the composition of traffic queues due to a random change in the traffic flow and its impact on emissions and the traffic capacity of intersections. This study found that the presence of various groups of vehicles and their position in the queue can reduce the traffic capacity by up to 70% and increase the growth of harmful emissions by 14 fold.

Keywords: vehicle queue structure; pollutant emissions; fuzzy logic method; intelligent vision

MSC: 03B52; 94D05; 92B20; 93A30; 91C20



Citation: Shepelev, V.; Glushkov, A.; Slobodin, I.; Balfaqih, M. Studying the Relationship between the Traffic Flow Structure, the Traffic Capacity of Intersections, and Vehicle-Related Emissions. *Mathematics* **2023**, *11*, 3591. <https://doi.org/10.3390/math11163591>

Academic Editor:

Aleksandr Rakhmangulov

Received: 6 July 2023

Revised: 14 August 2023

Accepted: 17 August 2023

Published: 19 August 2023



Copyright: © 2023 by the authors. Licensee MDPI, Basel, Switzerland. This article is an open access article distributed under the terms and conditions of the Creative Commons Attribution (CC BY) license (<https://creativecommons.org/licenses/by/4.0/>).

1. Introduction

The rapid development of the global economy and increasing per capita consumption have inevitably affected the urban environment. The transport sector is a significant contributor to air pollution. Just in Europe, approximately 238,000 people died prematurely from the harmful effects of automobile emissions [1]. Residents living close to large road arteries and junctions are exposed to particularly strong and constant pollution [2]. A huge number of vehicles congest the highways, especially at intersections.

Congestion leads to many negative economic (vehicle wear, fuel consumption, increased travel time), environmental (increase in harmful emissions), and psychological (increasing noise, driver stress, accident rate) factors. The numerous reasons for congestion can be conditionally divided into permanent (such as the geometry of the road structure, inconsistent traffic light operation, parked cars causing interferences) and random, including traffic accidents, weather conditions, and repairs.

Congestion control will certainly have a positive impact on air quality. Numerous vehicle emission models help assess environmental “hotspots”. These models can quantify air quality, which is essential for optimizing the effectiveness of traffic management.

Modeling requires a huge number of input parameters that closely interact with each other. Models with real-time data receipt are relevant now. Street video surveillance provides a suitable information flow that can be processed by neural networks with high speed and accuracy.

The urban traffic flow is very diverse and contains vehicles of various types and dimensions. Therefore, the actual air quality condition at a signal-controlled intersection is a complicated task with many different aspects.

Many works study the traffic capacity of signal-controlled intersections and build models to assess and forecast traffic-related emissions. However, there are no works assessing road traffic parameters and quantifying emissions dynamically. Further, our paper considers an approach to numerically determining the set of basic parameter estimates of a heterogeneous traffic flow.

This paper presents a detailed study of intelligent neural networks based on computer vision that analyzes traffic patterns at a specific intersection. Although the analysis considers the impact of variations in the traffic structural composition on emissions and traffic capacity, its applicability goes beyond the particular studied intersection. In particular, we study how changes in the vehicle composition affect the efficiency of intersections and increase harmful emissions. Using a combination of fuzzy logic approaches and Gaussian spline distribution functions, we highlight the variability of these relationships and emphasize the need for further exploring the balance between mobility and air quality. Ultimately, our findings point to the potential benefits of implementing intelligent traffic management strategies to optimize urban mobility while mitigating negative environmental impacts.

This paper is structured as follows: Section 2 reviews literature related to the traffic capacity of signal-controlled intersections and the main models of vehicle-related emissions. The intellectual vision method used to form the initial database is presented in Section 3. Section 4 analyzes the structure of the vehicle queue at signal-controlled intersections, based on which the relationship between intersection capacity and various vehicle types is presented in Section 5. Section 6 analyzes vehicle-related harmful emissions with changes in the queue structure, and Section 7 estimates the amount of vehicle-related emissions at signal-controlled intersections using fuzzy logic methods. Section 8 provides some discussions on this subject and the conclusions are presented in Section 9.

2. Literature Review

Traffic capacity (TC) is an essential performance indicator of a signal-controlled intersection [3–5]. The TC of intersections is critical for evaluating the performance of the road network in general. Many methods have been proposed for assessing and measuring the TC of signal-controlled intersections and many models for optimizing traffic at intersections have been developed [6–9]. However, most studies are based on the assumption that the traffic flow is homogeneous (all vehicles are standard) and are accepted for calculations according to the Highway Capacity Manual (HCM) as a passenger car equivalent (PCE) [10].

Over time, vehicle dimensions have changed and many correction factors should be revised [4]. All vehicles differ significantly in size and maneuverability, and therefore they move in the traffic flow at different speeds, which affects the TC of intersections [11].

The rapid development of video data recognition and processing technologies enabled the real-time assessment of the traffic flow characteristics on highways and intersections. Such valuable information is necessary for taking various measures to reduce and prevent congestions.

In paper [12], the authors proposed an approach for real-time measurement of the vehicle queue and congestion density at a signal-controlled intersection using an ultrasonic sensor node. Pandian et al. [13] studied the influence of the traffic flow composition on

TC on highways and presented a model to quickly assess the impact of various vehicle types on TC, ignoring the vehicle equivalence coefficient. The authors found that the TC of a highway decreases if there are buses, trucks, and other large vehicles in the flow of passenger cars. At the same time, the TC of a highway increases with an increase in the percentage of motorized two-wheeled vehicles.

Dhamaniya et al. [14] measured traffic flow density in mixed traffic conditions from the ratio of speed, flow, and density, and a rationale was provided for changes in speed depending on the traffic flow structure and traffic density.

The presence and movement of heavy vehicles (for passenger and bulky cargo transportation) on urban highways inevitably affects TC. In [15], Singh and Santhakumar used data obtained by an infrared sensor and found that the traffic flow speed is significantly reduced due to the low speed of heavy vehicles, especially when they cluster. Observations of a vehicle queue at a signal-controlled intersection in [16] showed that its length and delay time depend on the vehicle composition in the queue.

The quality of urban air depends on many factors, with vehicle exhaust gases exerting the largest influence [17,18]. The volume and composition of exhaust gases depend on the characteristics of traffic, the configuration of streets, and the number and types of vehicles [13]. Particularly unfavorable situations are found within intersections. The dispersion of vehicle-related harmful emissions is especially complicated when high-rise buildings surround intersections. Yassin et al. [19] used a computational fluid dynamics (CFD) model to establish that the concentration of harmful emissions at regular intersections is higher than at T-shaped and oblique intersections.

Woodward et al. [20] comprehensively studied the dispersion of traffic-related harmful emissions in cities. They concluded that when the vehicle is moving, harmful emissions are dispersed faster due to the turbulence caused by road traffic. In the intersection zone, where vehicles are not moving (or moving slowly), their engines are idling (at low speeds) and emissions are produced, respectively, there is no turbulence from the traffic flow and harmful emissions are dispersed very slowly (especially in calm weather). Therefore, in the intersection area, the concentration of harmful emissions is much higher than within other road sections.

A greater number of buses tends to increase mixed traffic conditions, especially in urban areas with actively developing public transport. The priority movement of buses through signal-controlled intersections creates interference and delays for other vehicles, which increases fuel consumption and harmful emissions [21].

The characterization of vehicle-related exhaust gas emissions carried out by Jaikumar et al. [22] and Ritner et al. [23] showed that emissions at idle speed and when the vehicle is moving at cruising speed are much lower than those during rapid acceleration and deceleration.

Wang et al. [24] analyzed the factors affecting emissions from city buses. The authors used a backpropagation neural network (BPNN) to analyze multiple factors and concluded that such factors as delay time, location, and stops significantly affect emissions. At the same time, the speed and number of passengers weakly affected the volume of emissions.

The number of connected and autonomous vehicles (CAVs) has been increasingly growing on roads, which undoubtedly affects the traffic capacity of both highways and intersections. In [25], the authors found that the TC of an intersection with CAVs increases by 70% compared to human-driven vehicles.

A study on the impact of CAVs with a dynamic distributed routing algorithm on greenhouse gas emissions showed that the widespread introduction of CAVs significantly reduced emissions, since the routing system reduced traffic congestion [26]. However, despite this positive effect, there was a simultaneous increase in the cruising speed and acceleration, which increased NO_x emissions and led to areas with high NO₂ concentrations. Thus, compromises should be sought out between the effectiveness of traffic control and the dispersion of harmful emissions.

Many studies have found that particulate matter (PM) cause irreparable harm to living organisms up to cellular mutations. PM are emitted into the atmosphere with other harmful substances during the operation of gasoline and diesel engines [27]. Close attention should be paid to this type of harmful emissions, which mostly comes from vehicles.

PM emission assessment methods can be divided into laboratory measurements (using special instruments (optical aerosol monitor [28], photoacoustic device [29])), and measurements in real conditions using various models: Mobile Source Factor Model (MOBILE), Comprehensive Modal Emissions Model (CMEM), California Line Source Dispersion Model (CALINE) [30], Computer programs to calculate emission from road transport (COPERT) [31], Passenger Car and Heavy Duty Emission Model (PHEM) [32], Electronic Model of Population Activities (EMPA), and Modeling of Emissions and Consumption (MODEM) [33].

Instrumental measurements have limitations and cannot reflect reality, as they do not account for many factors of driving conditions. The developed models are focused on the micro level (a certain section of the road network), if there are available data for this segment and traffic conditions. The resulting estimate for the amount of vehicle-related emissions is obtained as an average, since the models assume that vehicles run on traditional fuel and vehicle-related emission factors for various types of vehicles are used. Emissions analysis can be improved by using the fuzzy logic methods that take into account the uncertainty and subjectivity of many factors inherent in complex environmental assessment.

Carbajal-Hernández et al. [34] presented a model for assessing the air condition quality based on a fuzzy inference system, which provides results which are more accurate and closer to true emissions.

Fuzzy modeling methods, using logical, numerical, linguistic information for analysis, have become widespread for forecasting complex processes, including environmental ones. For example, the authors [35] developed a model that combines neural and fuzzy methods to predict a pollution episode. The Index of agreement ranges from 75 to 90% when forecasting harmful emissions.

Combined models are used to improve the efficiency of forecasting. For example, in [36], researchers use the data preprocessing method, fuzzy theory, and an optimization algorithm.

Most studies of vehicle-related harmful emissions are focused either on measures to increase the TC in order to reduce the environmental load, or on the assessment and analysis of harmful emissions in the road network structure. We aim to fill this research gap. In our study, we estimate the amount of PM_{2.5} at signal-controlled intersections based on fuzzy logic methods and the relationship between PM_{2.5} emissions and the structure of the traffic flow queue in real time.

Our study unites several areas related to traffic management and environmental impact. The new approach includes studying the relationship between the structure of traffic flows, the traffic capacity of intersections, and vehicle-related emissions. Further, this article uses new methods, such as intelligent data extraction and interpretation, as well as fuzzy logic methods to analyze these relationships. These innovations provide valuable insights into the optimization of traffic flows and the reduction in vehicle-related emissions in urban environments. This study aims to improve the sustainability and efficiency of urban planning and transport systems.

3. Intelligent Vision and Initial Data Generation

A software system was developed to collect data on the traffic flow structure and pollutant emissions. It analyzes the video stream from the road network section using neural network technologies. We analyzed the intersection of Prospect Pobedy and Krasnoznamennaya street in Chelyabinsk, Russia using a free-access Intersvyaz camera (Figure 1) [37]. This intersection was chosen because of the fairly good camera angle that allows us to view several queues of vehicles, a short distance that provides good visibility and allows us to

detect and classify vehicles with high accuracy, and the absence of obstruction of view by poles and trees.



Figure 1. Photo of the intersection of Prospect Pobedy and Krasnoznamennaya street in Chelyabinsk, Russia from a surveillance camera [37].

We processed video recordings for 15 days during peak hours from 7:30 a.m. to 9:30 a.m. and from 17:00 p.m. to 19:00 p.m. We analyzed approximately 60 h of video data in total.

The YOLOv4 (You Only Look Once) [38] neural network was used to detect and classify vehicles. The classification includes:

- I—passenger cars;
- II—vans and minibuses up to 3.5 tons;
- III—trucks from 3.5 to 12 tons;
- IV—trucks over 12 tons;
- V—buses over 3.5 tons;
- Tram—trams.

The freely available Simple Online and Real-time Tracking (SORT) tracker [39] was used to track and identify vehicles. A checkerboard overlay was used to calibrate and eliminate the radial camera distortion. A perspective transformation matrix based on four reference points was used to determine the geographical coordinates of vehicles [40]. It converts the screen coordinates of an object into its longitude and latitude at the intersection. The obtained geographical coordinates are used to calculate the distance traveled and the average travel speed of vehicles.

Atmospheric emissions were calculated according to [41,42] for the following pollutants:

- CO—carbon monoxide;
- NO_x—the sum of nitrogen oxides (in terms of nitrogen dioxide);
- PM_{2.5};
- PM₁₀.

A functional zone was manually marked in the center of the intersection for calculations. We marked entry and exit zones with polygons and lines of points on the border of the functional zone. The points were placed approximately in the center of the lines in the section of the image in which vehicles can be tracked well to precisely determine the direction of movement. Each zone was named according to the cardinal directions: N, S, W, E for entry zones and _N, _S, _W, _E for exit zones. Each line was also named according to its zone and number (for example: N1, W2, _E3). To determine the entry and exit zone, we check if the object is in the polygon, and to determine the lane, we search for the point of

the corresponding zone which is closest to the trajectory of the object. Figure 2 shows the operation of the system at a marked intersection.

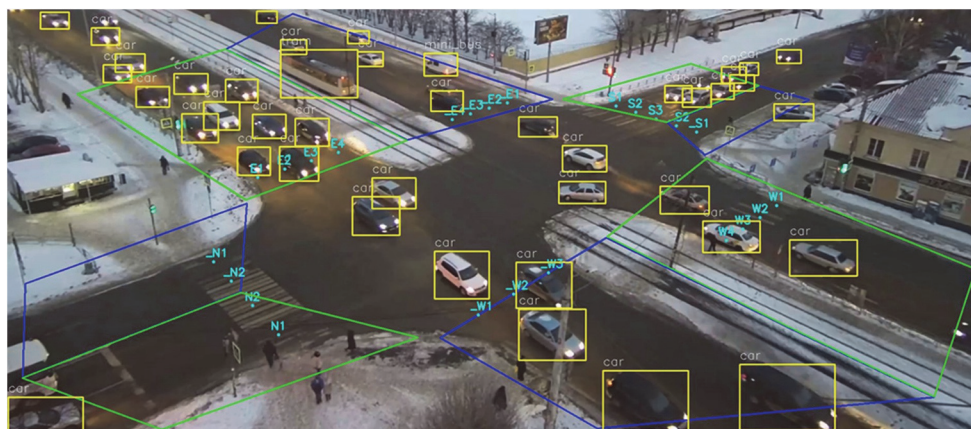


Figure 2. Marked image with zones and lines (green borders indicate entry zones; blue borders indicate exit zones. Yellow frames indicate vehicles detected by the neural network).

Throughout the object tracking period, each frame of its coordinates is stored in the detection queue. After the vehicle can no longer be tracked, the following parameters are calculated:

- line_in—entry lane;
- line_out—exit lane;
- millis_in—time in milliseconds when the vehicle was closest to the entry point;
- millis_out—time in milliseconds when the vehicle was closest to the exit point;
- speed—average speed in km/h within the functional zone;
- dist—distance in meters traveled inside the functional zone;
- stay—standing time in milliseconds within the functional zone;
- move—movement time in milliseconds within the functional zone;
- emis_CO, emis_NOx, emis_PM2.5, emis_PM10—emissions in grams produced by vehicles within the functional zone;
- emis_stay_CO, emis_stay_NOx, emis_stay_PM2.5, emis_stay_PM10—emissions in grams produced by vehicles during standing inside the functional zone;
- emis_move_CO, emis_move_NOx, emis_move_PM2.5, emis_move_PM10—emissions in grams produced by vehicles while driving inside the functional zone.

Using the video from the intersection, we measured the operating mode of the traffic light consisting of two main cycles:

1. The duration of the green signal is 48 s. The green signal is active for the following driving directions: W1_E1, W1_S1, W2_E2, W3_E3, W4_E4, W4_N2, E1_N1, E2_W1, E3_W2, E4_W3, E4_S2 (Figure 3);
2. The duration of the green signal is 34 s. The green signal is active for the following driving directions: N1_W1, N1_S1, N2_S2, N2_E4, S1_E1, S2_N1, S3_N2, S3_W3 (Figure 4).

The green light cycle is determined for vehicles when the vehicle moves into the functional zone. The number of the vehicle in its queue is also determined. Vehicles belong to the same queue if they have the same entry line. The sequence is determined according to the millis_in parameter within one cycle (the smaller this number, the earlier the vehicle is in the queue).

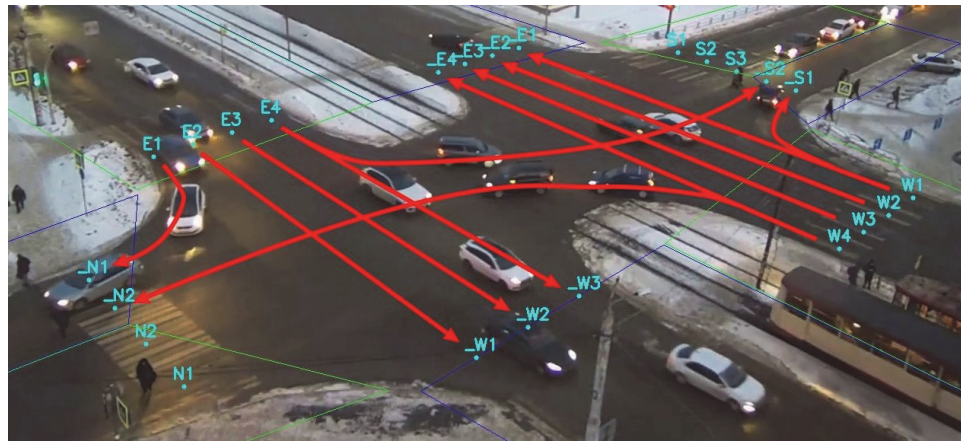


Figure 3. Driving directions (red lines with arrows) during the first traffic light cycle.

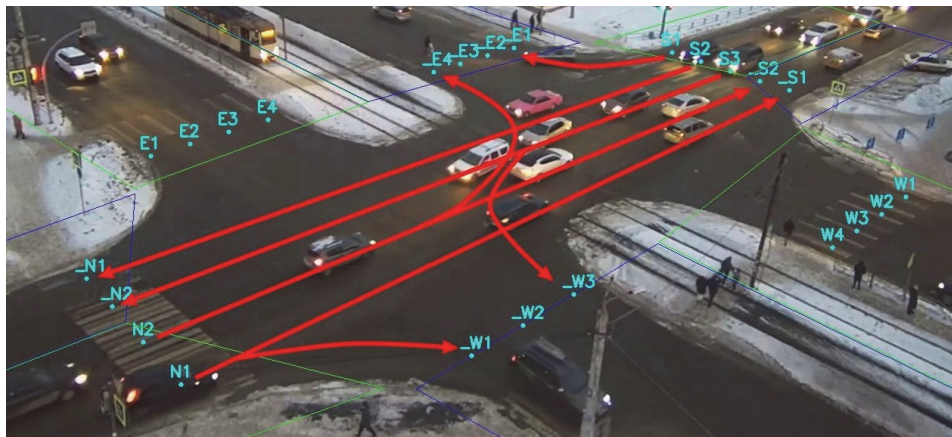


Figure 4. Driving directions (red lines with arrows) during the second traffic light cycle.

The system creates an “xlsx” file (Tables 1–3) with the following columns:

- “id”—vehicle identifier;
- “start signal”—start time of the green light cycle;
- “end signal”—end time of the green light cycle;
- “line in”—entry line;
- “line out”—exit line;
- “pos”—number in the queue;
- “category”—vehicle category;
- “time in”—time of entry into the functional zone;
- “time out”—time of exit from the functional zone;
- “speed”—average speed inside the functional zone (km/h);
- “dist”—distance traveled inside the functional zone (m);
- “duration”—time spent inside the functional zone (s);
- “stay”—standing time inside the functional zone (s);
- “move”—movement time inside the functional zone (sec);
- “sCO, sNO_x, sPM_{2.5}, sPM₁₀”—amount of CO, NO_x, PM_{2.5}, PM₁₀ emissions produced by vehicles during standing inside the functional zone (grams);
- “mCO, mNO_x, mPM_{2.5}, mPM₁₀”—amount of CO, NO_x, PM_{2.5}, PM₁₀ emissions produced by the vehicles while driving inside the functional zone (grams);
- “tCO, tNO_x, tPM_{2.5}, tPM₁₀”—total amount of CO, NO_x, PM_{2.5}, PM₁₀ emissions produced by vehicles inside the functional zone (grams).

Table 1. Data on the order of vehicle movement.

ID	Start Signal	End Signal	Line in	Line out	Pos	Category	Time in	Time out
73	07:30:46	07:31:37	E1	_N1	1	I	07:30:56	07:30:57
54	07:30:46	07:31:37	E2	_W1	1	I	07:30:51	07:30:54
77	07:30:46	07:31:37	E2	_W1	2	I	07:30:53	07:30:55
88	07:30:46	07:31:37	E2	_W1	3	I	07:30:57	07:30:59
96	07:30:46	07:31:37	E2	_W1	4	I	07:31:01	07:31:03
29	07:30:46	07:31:37	E3	_W2	1	I	07:30:50	07:30:53
75	07:30:46	07:31:37	E3	_W2	2	I	07:30:53	07:30:55
72	07:30:46	07:31:37	E3	_W2	3	I	07:30:54	07:30:56
80	07:30:46	07:31:37	E3	_W2	4	I	07:30:56	07:30:58
89	07:30:46	07:31:37	E3	_W2	5	I	07:30:59	07:31:01
130	07:30:46	07:31:37	E3	_W2	6	I	07:31:28	07:31:30
134	07:30:46	07:31:37	E3	_W2	7	I	07:31:31	07:31:32
140	07:30:46	07:31:37	E3	_W2	8	I	07:31:35	07:31:36
144	07:30:46	07:31:37	E3	_W2	9	I	07:31:37	07:31:38
63	07:30:46	07:31:37	E4	_W3	1	I	07:30:48	07:30:50
69	07:30:46	07:31:37	E4	_W3	2	I	07:30:50	07:30:52
28	07:30:46	07:31:37	W1	_S1	1	I	07:30:55	07:30:57
82	07:30:46	07:31:37	W1	_S1	2	I	07:30:59	07:31:01
94	07:30:46	07:31:37	W1	_S1	3	I	07:31:03	07:31:05
100	07:30:46	07:31:37	W1	_S1	4	I	07:31:06	07:31:08
105	07:30:46	07:31:37	W1	_S1	5	I	07:31:09	07:31:10
112	07:30:46	07:31:37	W1	_S1	6	I	07:31:11	07:31:14

Table 2. Data on vehicle movement parameters.

ID	Speed	Dist	Duration	Stay	Move
73	15.4	2.3	1.03	0	1.03
54	24.4	17.7	2.49	0	2.49
77	32.8	18.4	2.20	0	2.20
88	35.8	19.2	2.00	0	2.00
96	37.8	19.9	1.92	0	1.92
29	27.5	17	2.57	0	2.57
75	34.1	19.2	2.22	0	2.22
72	37.6	20.4	1.92	0	1.92
80	43.6	19.6	1.67	0	1.67
89	44.0	20.6	1.68	0	1.68
130	50.4	19.2	1.45	0	1.45
134	52.2	19.1	1.40	0	1.40
140	53.5	21.6	1.48	0	1.48
144	53.9	17.4	1.32	0	1.32
63	32.5	21.4	2.39	0	2.39
69	37.4	22.3	2.32	0	2.32
28	12.3	4.2	1.84	0	1.84
82	10.8	6.4	2.67	0	2.67
94	14.7	6.7	1.67	0	1.67
100	15.6	4.2	1.49	0	1.49
105	16.5	5	1.44	0	1.44
112	12.9	4.2	2.39	0	2.39

Table 3. Emission data.

ID	sCO	sNOx	sPM2.5	sPM10	mCO	mNOx	mPM2.5	mPM10	tCO	tNOx	tPM2.5	tPM10
73	0	0	0	0	0.00250	0.00091	0.00003	0.00007	0.00250	0.00091	0.00003	0.00007
54	0	0	0	0	0.01594	0.00584	0.00018	0.00048	0.01594	0.00584	0.00018	0.00048
77	0	0	0	0	0.01545	0.00566	0.00018	0.00047	0.01545	0.00566	0.00018	0.00047
88	0	0	0	0	0.01487	0.00545	0.00017	0.00045	0.01487	0.00545	0.00017	0.00045
96	0	0	0	0	0.01342	0.00492	0.00015	0.00041	0.01342	0.00492	0.00015	0.00041
29	0	0	0	0	0.01525	0.00559	0.00018	0.00046	0.01525	0.00559	0.00018	0.00046
75	0	0	0	0	0.01522	0.00558	0.00018	0.00046	0.01522	0.00558	0.00018	0.00046
72	0	0	0	0	0.01375	0.00504	0.00016	0.00042	0.01375	0.00504	0.00016	0.00042
80	0	0	0	0	0.01061	0.00389	0.00012	0.00032	0.01061	0.00389	0.00012	0.00032
89	0	0	0	0	0.01113	0.00408	0.00013	0.00034	0.01113	0.00408	0.00013	0.00034
130	0	0	0	0	0.00519	0.00190	0.00006	0.00015	0.00519	0.00190	0.00006	0.00015
134	0	0	0	0	0.00516	0.00189	0.00006	0.00015	0.00516	0.00189	0.00006	0.00015
140	0	0	0	0	0.00584	0.00214	0.00006	0.00017	0.00584	0.00214	0.00006	0.00017
144	0	0	0	0	0.00470	0.00172	0.00005	0.00014	0.00470	0.00172	0.00005	0.00014
63	0	0	0	0	0.01807	0.00662	0.00021	0.00055	0.01807	0.00662	0.00021	0.00055
69	0	0	0	0	0.01654	0.00606	0.00019	0.00050	0.01654	0.00606	0.00019	0.00050
28	0	0	0	0	0.00495	0.00181	0.00005	0.00015	0.00495	0.00187	0.00005	0.00015
82	0	0	0	0	0.00760	0.00278	0.00009	0.00023	0.00760	0.00278	0.00009	0.00023
94	0	0	0	0	0.00787	0.00288	0.00009	0.00024	0.00787	0.00288	0.00009	0.00024
100	0	0	0	0	0.00457	0.00167	0.00005	0.00014	0.00457	0.00167	0.00005	0.00014
105	0	0	0	0	0.00545	0.00199	0.00006	0.00016	0.00545	0.00199	0.00006	0.00016
112	0	0	0	0	0.00486	0.00178	0.00005	0.00014	0.00486	0.00172	0.00005	0.00014

4. Analysis of the Vehicle Queue Structure

The acquired large array of initial data of 188,619 entries of vehicles moving in the intersection in all possible driving directions allows us to obtain statistically reliable results necessary to answer many basic questions regarding the traffic flow structure.

First, we should determine the characteristics of a homogeneous traffic flow consisting of vehicles of the first group (*TV-1*) (passenger cars) that prevail in the traffic flows of the analyzed intersection. Then, we should analyze the impact on these characteristics of vehicles belonging to other groups: group 3 (*TV-3*) (trucks weighing from 3.5 to 12 tons); 4 (*TV-4*) (trucks weighing over 12 tons) and 5 (*TV-5*) (buses weighing over 3.5 tons). Notably, this study does not consider group 2 (*TV-2*) vehicles (vans and minibuses weighing up to 3.5 tons), since previous study [43] have shown that they do not significantly change the temporal characteristics of the flow of vehicles belonging to the first group.

4.1. Intervals between Vehicles

The common interval between moving vehicles in a continuous traffic flow is 2 s. However, we are interested in a specific traffic flow: a queue of vehicles that start moving after a complete stop at a red light. We formed a sample of the initial data consisting of 22 strictly continuous flows of passenger cars. We restricted the interval between the first ten cars to no more than 5 s as a criterion for the continuity of the traffic flow. This should reject entries with freely moving vehicles that were not in the vehicle queue at the signal-controlled intersection. A sample of 22 entries, 10 cars each, proved to be sufficient, since in practice its increase from approximately the 15th entry did not change the general trend.

Figure 5 shows the average value of the intervals between cars (I_1), depending on their position in the queue of vehicles that resume movement after coming to a complete stop.

Comparing the average values by the parametric one-sample Student’s *t*-test (IBM SPSS Statistics 20 package) showed that from the third interval on, there is no statistically significant deviation of the intervals between moving vehicles from the generally accepted level of 2 s (the value of 34% significantly exceeds the permissible level of 5%). The calculations allow us to accept this interval as valid for any vehicle queue size and use it for further analyses.

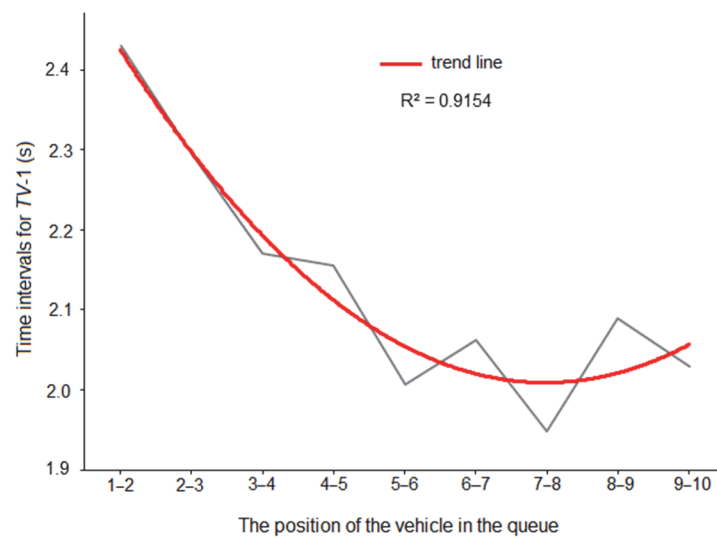


Figure 5. The change in the time interval from the position of the car in the queue.

4.2. Maximum Vehicle Queue Size

The maximum size of the queue of passengers is estimated based on the assumption of a saturation flow, when the traffic flow consisting of only passenger cars moves continuously without major time intervals between vehicles during the entire cycle of the green light. The initial data array includes traffic flows recordings from 15 business days in two blocks (morning and evening). There are 30 observation blocks in total, with an average of 6000 entries per block. The maximum number of vehicles passing through on a green light is determined in each block, as shown in Figure 6.

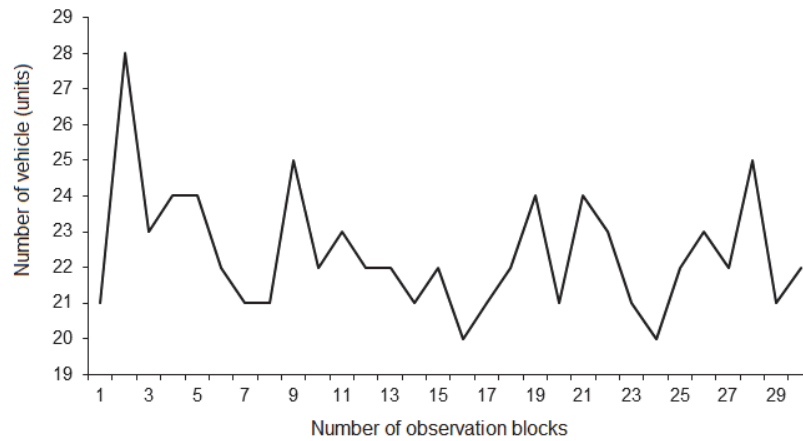


Figure 6. Maximum traffic capacity in 30 observation blocks.

Descriptive statistics revealed that maximum queue size ranged from 20 to 28 cars; the mathematical expectation is 22.4 cars with a standard deviation of 1.7 cars. The variation coefficient is 7.6%, which characterizes the high level of traffic flow stability during all 15 observation days.

A reasonable verification is grounded on the calculation of the maximum traffic capacity of the intersection, based on the duration of the green traffic light signal (51 s) and the average interval between TV-1 (2.1 s). We obtain 24.3 cars. Taking into account the natural delays at the beginning and end of the traffic light cycle expressed in a decrease in the traffic capacity by one car at the beginning and end of the cycle, we obtain the same estimate of the maximum traffic capacity of 22 cars.

Thus, the traffic capacity is assumed to be 22 TV-1 driving straight ahead for a signal-controlled intersection with a green light cycle of 51 s. Taking into account the assumption

of the saturation flow, we take the value of the maximum queue size that passes through the intersection during the green light cycle, also equal to 22 vehicles. This queue size will be used as a base value in our further calculations.

4.3. Vehicle Acceleration Dynamics

4.3.1. The TV-1 Group

The speeds of vehicles leaving the intersection were recorded in the array of initial data, which allows us to determine changes in speed depending on the position of the vehicle in the queue formed at the red light. The accepted size of this queue is 22 vehicles, according to the calculations above.

Out of 30 blocks of 6000 entries (15 days, morning and evening), we selected entries in the initial data that corresponded to a queue of up to 17 vehicles passing through the intersection, since a larger traffic flow breaks its continuity. Out of ten blocks of initial data, we selected 22 entries including speeds from 12 to 17 vehicles for a total of 220 entries. A further increase in the sample after the 6th block did not significantly change the established trend; therefore, processing was limited to ten blocks. Figure 7 shows the actual dynamics of the speed of vehicles leaving the intersection, depending on their position in the queue (actual TV-1).

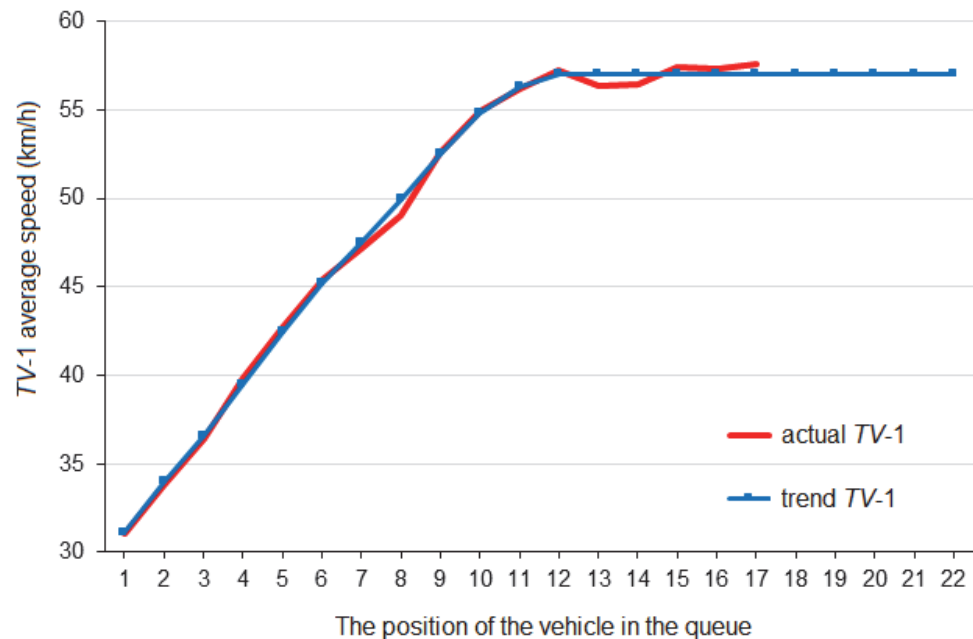


Figure 7. The actual speed and speed trend of TV-1 upon exiting the intersection.

Our further analysis compares the speeds for all major groups of vehicles, so it is advisable to smooth and extrapolate this trend to the entire maximum queue size. The smoothing criterion is the minimization of the standard deviation error, and extrapolation prolongs the trend for the entire maximum possible queue of 22 vehicles at this intersection. The results of this additional processing of vehicle speeds averaged over the sample are also shown in Figure 7 (trend TV-1).

This upward trend in the speed of low-inertia vehicles at the exit from the intersection is in good agreement with a priori estimates. The first car accelerates from the stop line to the exit to 32 km/h; the following cars evenly increase their speed to close to the maximum permitted speed of 60 km/h; and then the traffic flow of the entire queue moves uniformly at a speed of 57 km/h. This trend in the speed of passenger cars is taken as a basis for our further comparison with vehicles of other classification groups.

4.3.2. The TV-3 Group

As with the other groups, out of 30 blocks of 6000 entries on average (15 days, morning and evening), we selected entries in the initial data that corresponded to queues of up to 15 cars containing one TV-3 vehicle at different positions in the queue passing through an intersection. We could not record entries with a large queue because of the discontinuity of the traffic flow and the decrease in the queue due to the presence of bulky vehicles from TV-3.

A total of 73 satisfactory entries were selected for a queue of up to 15 vehicles, which contained only one group 3 (TV-3) vehicle at various positions in the queue. The remaining vehicles in the queue are from TV-1. In light of their low inertia, their position in front of TV-3 vehicles does not affect the acceleration of individual trucks.

However, a relatively small sample demonstrated the main trend in the dynamics of the acceleration speed of vehicles (actual TV-3), as shown in Figure 8 with an approximate trend line for the maximum queue (trend TV-3). Figure 8 also presents the previous trend in the speed dynamics for passenger cars (trend TV-1).

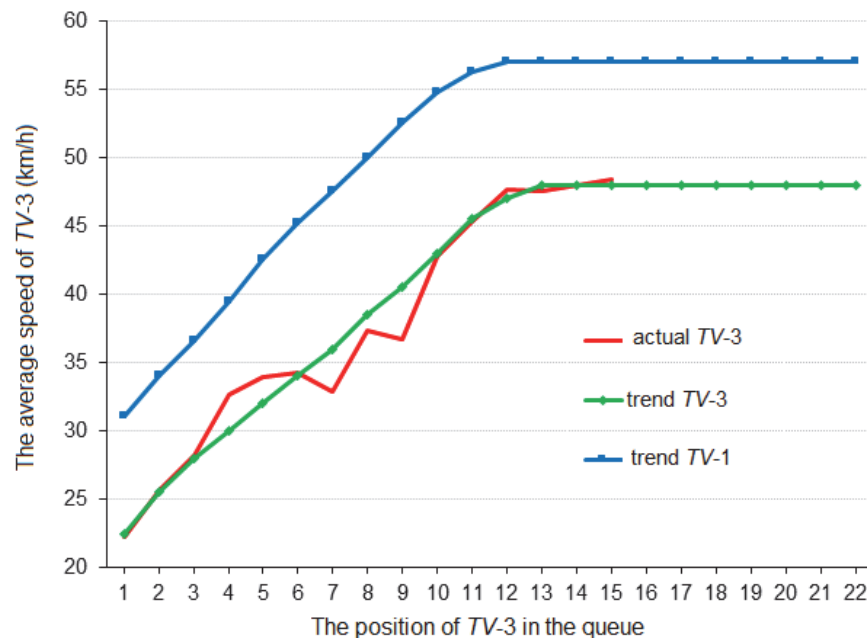


Figure 8. The actual speed and speed trend of TV-3 group at the exit from the intersection.

The minimization of the mean square deviation error is taken as the smoothing criterion, and extrapolation prolongs the trend for the entire maximum possible queue of 22 vehicles at an intersection. The revealed trend in the speed dynamics of TV-3 group also agrees well both with its a priori estimate. TV-3 group shows lower speeds and slightly slower acceleration for inertial trucks compared to passenger cars.

4.3.3. The TV-4 Group

The fourth group of vehicles (TV-4) consists of trucks weighing over 12 tons, which have high inertia in dynamic driving modes. Out of 30 blocks of 6000 entries on average (15 days, morning and evening), we selected entries which corresponded to a queue of up to 15 vehicles passing through the intersection, given that the traffic flow is continuous, with one TV-4 group vehicle at different positions in the queue. A total of 87 satisfactory entries were selected, each containing no more than 15 vehicles.

The actual dynamics of the acceleration speed of TV-4 generally coincide with the speed dynamics in the third group (actual TV-3), as shown in Figure 9, and the approximating trend line for the maximum queue size is almost the same (trend TV-3, TV-4). This result was anticipated, since with an increase in the total mass of group 4 vehicles, the

power of their engines also increases, and the movement nature of inertial trucks of both the third and fourth groups should be similar.

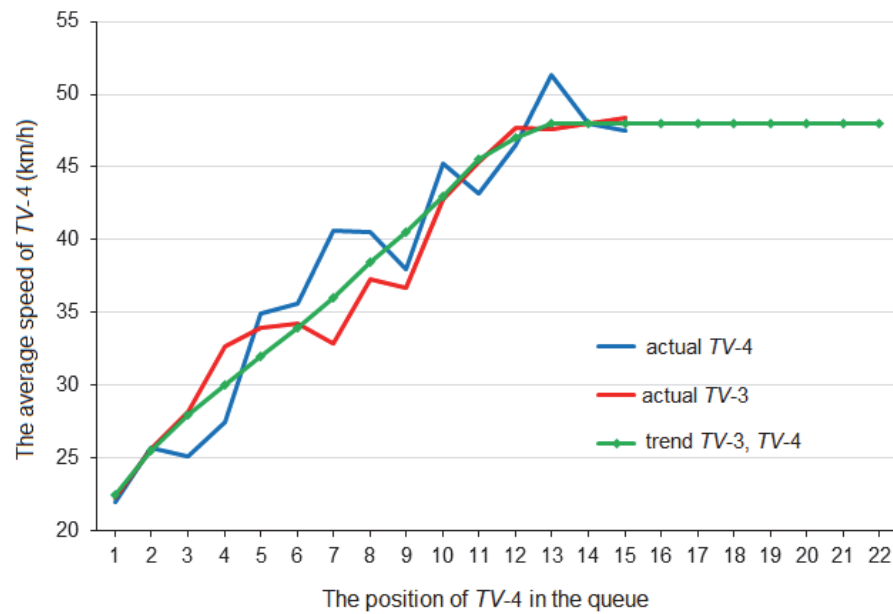


Figure 9. The actual speed and speed trend of TV-4 group at the exit from the intersection.

4.3.4. The TV-5 Group

The fifth group of vehicles (TV-5) consists of buses weighing over 3.5 tons generally used for passenger transportation. This should essentially affect the smoother overall acceleration trend.

Out of 30 blocks of 6000 entries on average (15 days, morning and evening), we selected entries which corresponded to a queue of up to 15 vehicles passing through the intersection, given that the traffic flow is continuous, with one TV-5 vehicle at different positions in the queue. A total of 73 satisfactory entries were processed, each containing no more than 15 vehicles.

A sample demonstrated the main trend in the dynamics of the acceleration speed of vehicles (actual TV-5), shown in Figure 10 with an approximating trend line for a queue of 22 vehicles (trend TV-5). Additionally, Figure 10 shows the previous trend in the speed dynamics for passenger cars (trend TV-1).

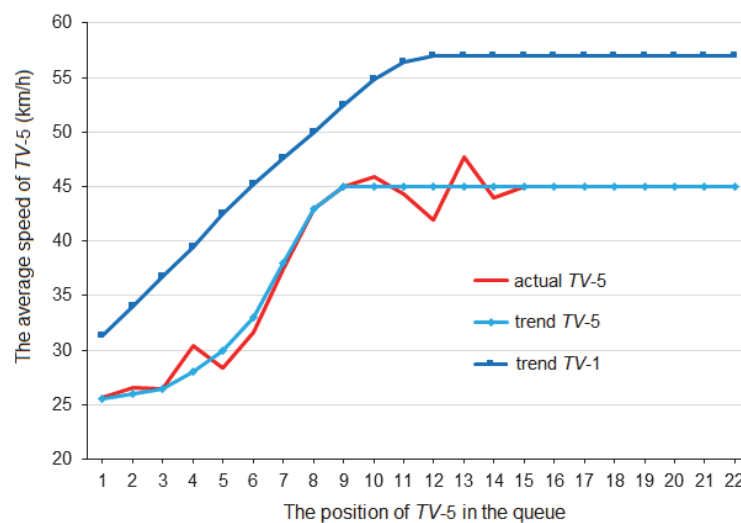


Figure 10. The actual speed and speed trend of TV-5 group at the exit from the intersection.

As anticipated, the speed of buses changes unevenly during acceleration, and the maximum speed is lower than that of vehicles from other groups.

Figure 11 compares all trends in the speed dynamics of vehicles from different groups. Passenger cars and trucks have the same type of acceleration, while the dynamic nature of acceleration of buses fundamentally differs; this can be explained by the large passenger capacity of buses.

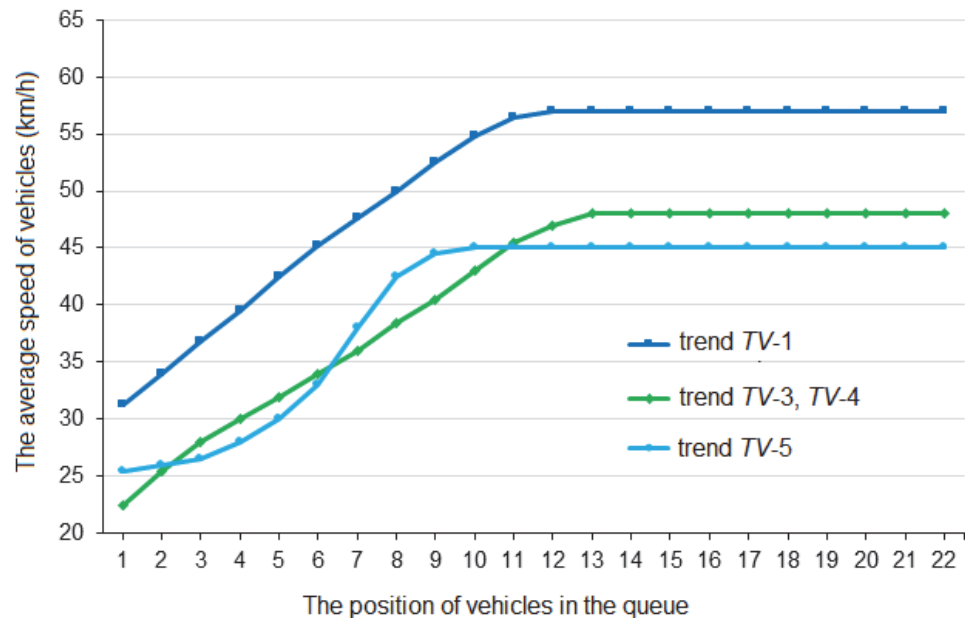


Figure 11. Speed trends of vehicles of different groups at the exit from the intersection.

These selective statistical characteristics of vehicles of different groups will be used in further calculations to compare the traffic capacity of a signal-controlled intersection and to estimate pollutant emissions when the queue structure varies.

5. Analysis of the Intersection Capacity with Changes in the Vehicle Queue Structure

The intersection capacity will decrease if there is a vehicle of another group in the queue of passenger cars. In this case, the last passenger car in the queue will not move according to its own speed profile (see Figure 11), but according to the profile of the vehicle of another group. Moreover, the position of this vehicle in the queue does not have any impact; only its presence is decisive. Based on this assumption, let us estimate the decrease in the intersection capacity if there are vehicles from groups 3, 4, and 5 in the queue.

5.1. Passenger Cars through the Intersection

The base value for estimating the decrease in the traffic capacity will be the time for the last passenger car to pass through the intersection if there are no vehicles of other groups in the queue. Numerical constants for calculations are:

- The time of the green light $T_0 = 51$ s;
- Intersection width $S_0 = 19.5$ m;
- The distance from the stop line to the area of the intersection itself $D_{sl} = 9$ m.

Based on the statistical processing of a sample of 120 entries for this intersection, we determined:

- The average length of a passenger car, $L_{pc} = 4.5$ m;
- The distance between cars in the queue, $D_q = 2.7$ m.

The Formulas for determining individual terms for the time the last car in the queue passes the intersection area are as follows. For the first position in the queue, as of reaching the center of the intersection, the acceleration time (t_1) is:

$$t_1 = \frac{2(S_0 + 0.5D_{sl})}{V_1}, \tag{1}$$

where V_1 is the acceleration speed of the first car.

For subsequent vehicles in the queue (21 cars), which both continue to accelerate and move at a constant speed, the additional time (t_i) is determined at the distance of the interval between cars equal to the sum ($L_{pc} + D_q$):

$$t_i = \frac{2(L_{pc} + D_{sl})}{V_{i-1} + V_i}. \tag{2}$$

The total time for the last car in the queue to pass through the intersection area determined by the considered algorithm is equal to $T_{t1} = 15.3$ s (for $TV-1$), which is much less than the time of the green light $T_0 = 51$ s. This is explained by the delayed start of each vehicle (t_d) in the queue; and the calculations give it an average estimate according to the following ratio:

$$t_d = \frac{T_0 - T_{t1}}{21}. \tag{3}$$

5.2. Queue with One Vehicle of Other Groups

If there is one vehicle in the queue of the third or fourth group with an identical traffic schedule in the intersection area (see Figure 12), similar calculations using Formulas (1) and (2) show the overall increase in the travel time of the last vehicle in the queue up to $T_{t34} = 19.9$ s, and if there is one vehicle of the fifth group in the queue—up to $T_{t5} = 19.4$ s.

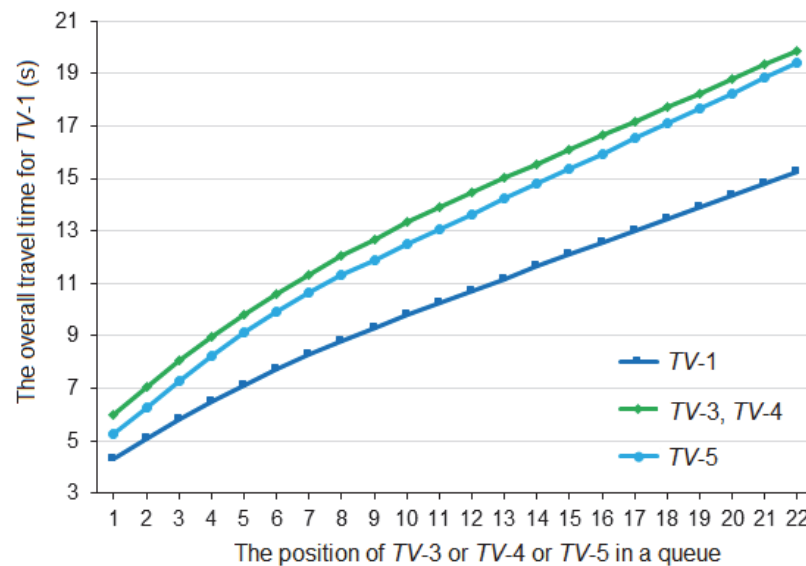


Figure 12. The time needed to pass the intersection by a queue of vehicles.

Figure 12 presents the corresponding accumulation graphs of the overall travel time for the queue of passenger cars ($TV-1$), if there is one vehicle in the queue from other transport groups ($TV-3$ or $TV-4$; $TV-5$). The accumulation dynamics depends on the position of the vehicle in a queue of 22 cars.

Taking into account the pre-defined time interval between passenger cars $I_1 = 2.1$ s, as well as the generally accepted coefficients for reducing vehicles to $TV-1$:

- $k_3 = 3$ for reducing $TV-3/TV-1$;
- $k_4 = 4$ —for $TV-4/TV-1$;

- $k_5 = 2.5—TV-5/TV-1$.

We can estimate the decrease in the intersection capacity if there is one vehicle of another category in the traffic flow of passenger cars.

The general estimation algorithm (%) P_{ri} for vehicles of the i -th group is determined by the formula:

$$P_{ri} = \frac{22 - \frac{T_{ii}-t_1}{I_1} - (k_i - 1)}{22} \cdot 100\%, \tag{4}$$

where the first difference $(T_{ii}-t_1)/I_1$ determines the decrease in the traffic capacity because of the slowdown of cars ($TV-1$) moving according to the pace of vehicles of the i -th group; the second difference $(k_i - 1)$ determines the decrease in the traffic capacity by the reduction coefficient for the vehicle of the i -th group.

The calculations give the following decrease in the traffic capacity P_{ri} when there is only one vehicle of another group in the queue:

- for $TV-3$: $P_{r3} = 81.8\%$;
- for $TV-4$: $P_{r4} = 77.3\%$;
- for $TV-5$: $P_{r5} = 84.1\%$.

5.3. Queue with Several Vehicles of Other Groups

With an increase in the number of other vehicles of any group in the queue, formula (4) changes as follows:

$$P'_{ri} = \frac{22 - \frac{T_{ii}-t_1}{I_1} - N_i(k_i - 1)}{22} \cdot 100\%, \tag{5}$$

where N_i is the number of vehicles of one i -th group in the queue of passenger cars.

Figure 13 a graph of the relationship between decrease in the traffic capacity P'_{ri} and an increase in the queue of vehicles of any one group.

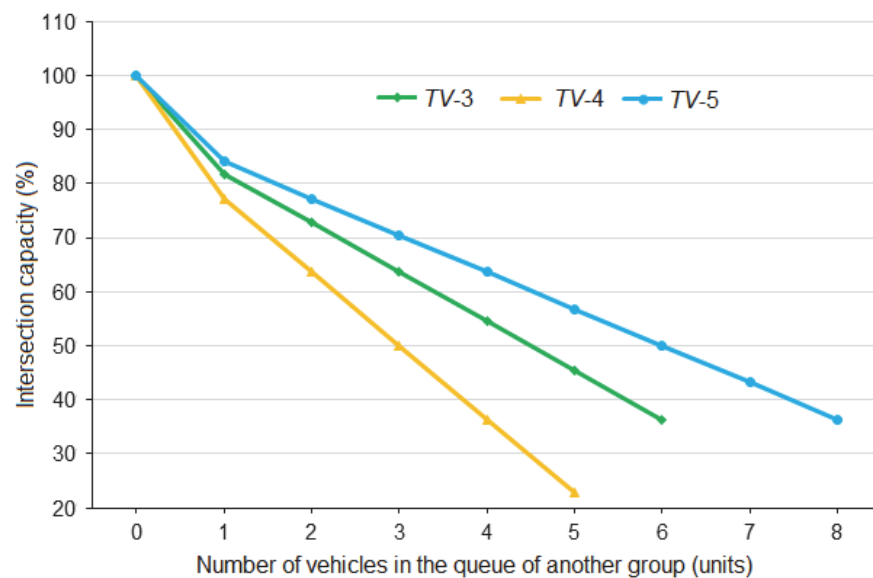


Figure 13. Intersection capacity with vehicles of various groups in the queue.

With the maximum increase in the number of vehicles of other groups in the queue, the intersection capacity drops below 40%. Moreover, this maximum number of other vehicles is limited: six vehicles for $TV-3$ group; five vehicles for $TV-4$ group; eight vehicles for $TV-5$ group.

It is also interesting to estimate the distribution field of the traffic capacity if there are simultaneously several vehicles of other groups in the queue of passenger cars. In view of

the proximity of the movement dynamics of groups *TV-3* and *TV-4*, we will consider the simultaneous impact of vehicles of groups *TV-3* and *TV-5* on the traffic capacity.

In this case, formula (4) is as follows:

$$P'_{3,5} = \frac{22 - \frac{T_{34}-t_1}{I_1} - N_3(k_3 - 1) - N_5(k_5 - 1)}{22} \cdot 100\%. \tag{6}$$

The distribution field shown in Figure 14 was built in Matlab R2015a (8.5.0.197613). The horizontal projection reflects the maximum possible combinations for the number of vehicles of two groups—*TV-3* and *TV-5*.

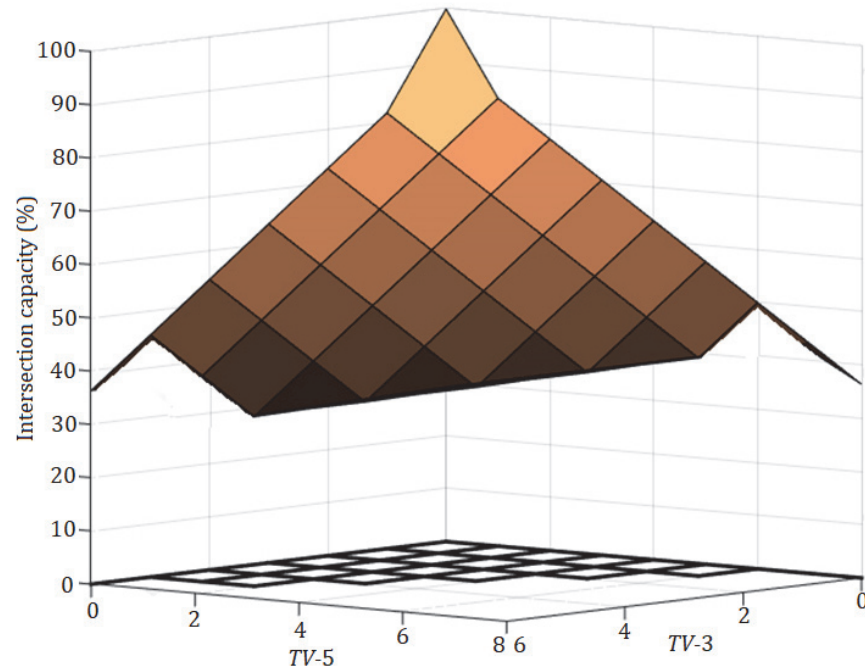


Figure 14. The distribution field of the intersection capacity if there are vehicles of two groups in the queue.

The maximum decrease in the intersection capacity to 31.8% is observed when there are five vehicles from *TV-3* group and two vehicles from *TV-5* group in the queue.

6. Analysis of Pollutant Emissions with Changes in the Vehicle Queue Structure

Vehicles are sources of many pollutants, both gases from vehicle-related exhaust gases and solid suspended microparticles from (besides soot emissions) the wear of tires, brake pads, roadway, and the lifting of settled dust from air vortices. Since microscopic PM2.5 particulate matter has the greatest impact on human health, we will evaluate how PM2.5 pollution changes with variations to the vehicle queue structure.

Regulated values of PM2.5 emissions and methods for calculating them from an arbitrary traffic flow are defined in national standards [41,42]. The calculations are divided into two parts: for vehicles moving freely at an arbitrary speed, and for vehicles stopping at a red light.

When calculating PM2.5 emissions for moving vehicles, we must account for the variable factor r_v , which determines the average vehicle speed and can be taken from standard Table 4 for a wide range of speeds. The speed limit for urban traffic does not exceed 60 km/h.

Table 4. Complete table of values for the correction factor r_v .

Speed (km/h)	r_v
5	1.4
10	1.35
15	1.3
20	1.2
25	1.1
30	1
35	0.9
40	0.75
45	0.6
50	0.5
60	0.3
70	0.4
80	0.5
100	0.65
110	0.75
120	0.9

In urban conditions, a vehicle constantly accelerates and decelerates within a particular road section, moving at an average speed determined by road conditions. Specific pollutant emission factors take into account this dynamic traffic nature. A 184-m zone was chosen to compare the amount of emissions from one passenger car while driving and idling. It takes into account the queue of 22 passenger cars and the measurement area at the intersection. It is assumed that a vehicle approaches the intersection during the red traffic light signal and stays at the intersection for a maximum of 37 s (the duration of the red traffic light signal). After that, the vehicle accelerates and leaves the intersection, driving a total of 184 m. An average driving speed of 5 km/h was taken to estimate the maximum possible amount of emissions during movement, so that the coefficient r_v (Table 4) was the maximum (1.4). Various idle times from 1 to 37 s are considered to calculate emissions during idling. The comparison result is shown in Figure 15. It can be seen from Figure 15 that, starting from 24 s of idling, the amount of emissions becomes larger than during movement. Since this estimate was made for a speed of 5 km/h, in a real situation the amount of emissions during movement will be less. Thus, even at low traffic flow speeds, vehicles waiting for the green traffic light signal at the intersection significantly affect the amount of harmful emissions.

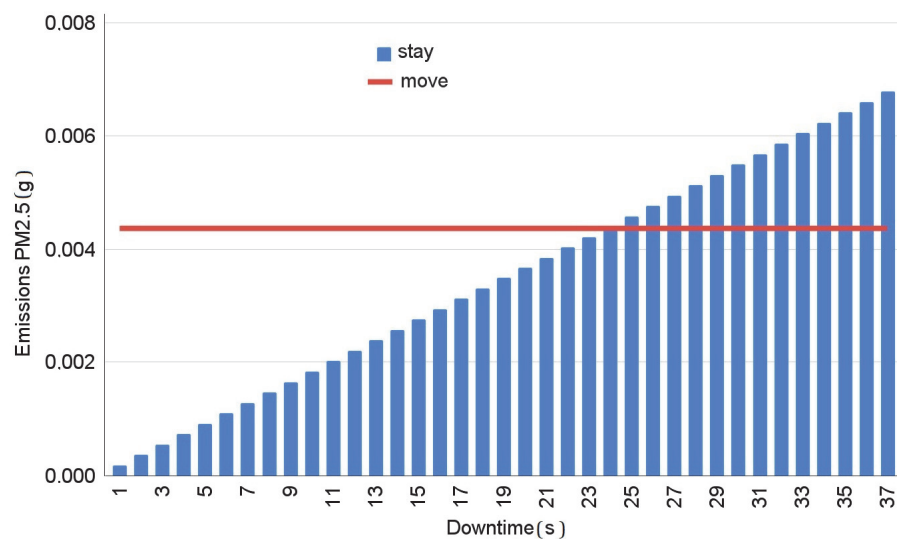


Figure 15. The amount of emissions from one passenger car in motion and at different idle times.

Taking into account this limitation, as well as the need to make calculations for an arbitrary vehicle speed, we performed trend approximation of this dependence reflected by formula (7):

$$r_v = a_0 + a_1 \cdot V + a_2 \cdot V^2 + a_3 \cdot V^3, \tag{7}$$

in which the numerical values of the coefficients a_i are given in Figure 16. Notably, the quality of the accepted approximation is high as confirmed by the multiple correlation factor $R^2 = 0.9988$.

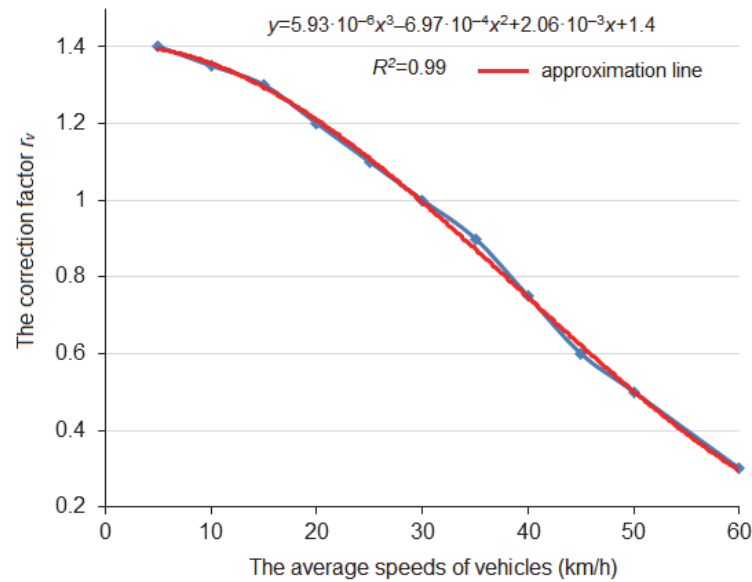


Figure 16. Trend approximation for the correction factor r_v .

The values of r_v for the average speeds of vehicles from various groups shown in Figure 11 will be also needed to calculate emissions. To this end, we converted the average speeds of vehicles of various groups into the correction factor r_v based on the developed trend approximation (Figure 11).

Figure 17 shows the results of this conversion for vehicles of various groups, depending on their position in the queue.

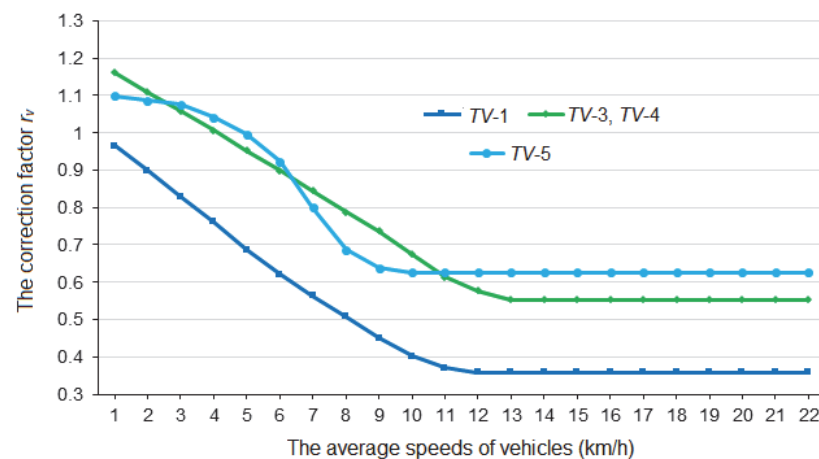


Figure 17. Correction factor r_v for the speeds of vehicles from various groups.

Comparative calculations of PM2.5 emissions for various groups of vehicles were analogous to the analysis of changes in the traffic capacity of a signal-controlled intersection. The Formulas of the national standard were converted by calculating PM2.5 emissions for an arbitrary traffic flow into any time interval for vehicles of a single queue. This significantly simplifies calculations and comparative assessments of pollutant emissions.

6.1. PM2.5 Emissions from Passenger Cars in the Intersection Area

The calculation of PM2.5 emissions from a full queue consisting of 22 passenger cars moving homogenously will provide a baseline estimate at subsequent variations in the traffic flow structure in the queue.

The national standard formula for calculating PM2.5 emissions at a red light (M_{Z1}) for one TV-1 vehicle is converted into:

$$M_{Z1} = P_Z \cdot M_{1z}, \tag{8}$$

where P_Z is the duration of the deceleration and acceleration phase of vehicles (8.6 s); M_{1z} is the PM2.5 emission factor for TV-1 vehicles, taking into account deceleration and acceleration time (0.011 g/min).

The national standard formula for calculating PM2.5 emissions at the green light M_{L1} for one TV-1 is converted into:

$$M_{L1} = \sum_{i=1}^{22} L_i \cdot M_{1l} \cdot r_{Vi}, \tag{9}$$

where i is the position number of the car in the queue; L_i is the distance by which the path of the car increases from the i -th position in the queue ($L_1 = 18.75$ m; $L_i = 7.2$ m for $i > 1$); M_{1l} is the running PM2.5 emission factor for TV-1 cars (0.0055 g/km); r_{Vi} is the correction factor for the i -th position of the vehicle in the queue (according to Figure 13).

Formula (8) estimates PM2.5 emissions for one TV-1 car: $M_{Z1} = 0.00158$ g. and $M_{L1} = 0.000397$ g. With a full queue of 22 cars, we obtain the total emissions $M_{S1} = 0.0434$ g. This estimate is taken as a baseline at subsequent variations in the traffic flow structure in the queue.

6.2. PM2.5 Emissions If There Is One Vehicle of Another Group in the Queue

A detailed analysis of the presence and location of one vehicle of another group in the queue of passenger cars revealed several interesting estimates in the variation in vehicle-related pollutant emissions.

1. Estimate 1.

Similar calculations by Formulas (8) and (9) for vehicles of other groups, with changes only in PM2.5 emissions factors M_{iz} and M_{il} , gave the increase in the total emissions from one vehicle of another group compared to emissions from a TV-1 vehicle:

- For one vehicle of TV-3 group, emissions increased 42 times;
- For one vehicle of TV-4 group, emissions increased 69 times;
- For one vehicle of TV-5 group, emissions increased 19 times.

2. Estimate 2.

Information on the percentage of running exhaust emissions in relation to acceleration-deceleration emissions determined for vehicles of various groups at an intersection will be very useful for urban traffic flow management. Calculations gave the following estimates:

- For a vehicle of TV-1 group—25.2%;
- For a vehicle of TV-3 group—89.9%;
- For a vehicle of TV-4 group—52.2%;
- For a vehicle of TV-5 group—78.6%

The obtained estimates indicate the importance of organizing traffic flows which do not come to a complete stop at a red light.

3. Estimate 3.

If there is one vehicle of another group (TV- i) in the queue of passenger cars (TV-1), it divides passenger cars into two flows according to emissions.

The first flow consists of vehicles moving ahead of the vehicle of the i -th group ($TV-1_i$). Their travel speed trend and the amount of PM2.5 emissions remain unchanged.

The second flow consists of vehicles moving behind the vehicle of the i -th group ($V-i_1$) according to its movement trend (see Figure 7). In this case, the emissions from cars of the first group increases.

So, running exhaust emissions, as determined by formula (8), increase:

- For one passenger car $TV-3_1/TV-1_3$ (or $TV-4_1/TV-1_4$)—47.4%;
- For one passenger car $TV-5_1/TV-1_5$ —53.3%.

The obtained estimates for the increase in the total emissions are much less:

- For one passenger car $TV-3_1/TV-1_3$ (or $TV-4_1/TV-1_4$)—9.5%;
- For one passenger car $TV-5_1/TV-1_5$ —10.7%.

This is because running exhaust emissions are much less than acceleration and deceleration emissions, which is also valuable information for traffic flow management.

4. Estimate 4.

The final estimate of PM2.5 emissions is total emissions from the entire queue of vehicles consisting of passenger cars and one vehicle of another group in an arbitrary place in the queue. Notably, a vehicle’s place in the queue is only critical for calculating the free movement of vehicles. In this approach, the Formulas for emissions from the entire queue are as follows.

PM2.5 emissions at the red light M_{Z1i} converts formula (8) (here, i is the group number of one vehicle that does not belong to $TV-1$):

$$M_{Z1i} = N_1 \cdot P_{1z} \cdot M_{1z} + 1 \cdot P_{iz} \cdot M_{iz}, \tag{10}$$

where N_1 is the number of passenger cars in the full queue if there is one vehicle of another group in it.

The formula for calculating PM2.5 emissions at the green light, in particular for a queue with one $TV-3$ vehicle M_{L13} , is converted into:

$$M_{L13} = N_{13} \cdot M_1 \cdot \sum_{i=1}^{22} L_i \cdot r_{V1i} + N_{31} \cdot M_1 \cdot \sum_{i=1}^{22} L_i \cdot r_{V3i} + 1 \cdot M_3 \cdot \sum_{i=1}^{22} L_i \cdot r_{V3i}, \tag{11}$$

where N_{13} is the number of passenger cars in the full queue located in front of the $TV-3$ vehicle and moving according to their own speed profile; N_{31} is the number of passenger cars in the full queue located after the $TV-3$ vehicle and moving according to its speed profile (taken into account by the correction factor r_{V3}).

The calculations are similar to Formula (11) for a queue of vehicles containing one vehicle from $TV-4$ or $TV-5$.

The calculations showed the following general trend in the relationship between PM2.5 emissions on the position of one vehicle of another group in the queue (see Figure 18).

If there is one vehicle of another group in the queue of passenger cars, PM2.5 emissions significantly increase. The relative estimates of excess emissions are as follows:

- If there is one $TV-3$ in the queue—276%;
- If there is one $TV-4$ in the queue—394%;
- If there is one $TV-5$ in the queue—172%.

Notably, the position of a vehicle of another group in the queue of passenger cars has little impact on the change in total emissions. The general trend is that the further the vehicle of another group is in the queue, the fewer passenger cars will be after it. Moving according to a different group’s speed profile increases PM2.5 emissions. This means that the further the vehicle of another group is in the queue, the less emissions the entire vehicle queue generates.

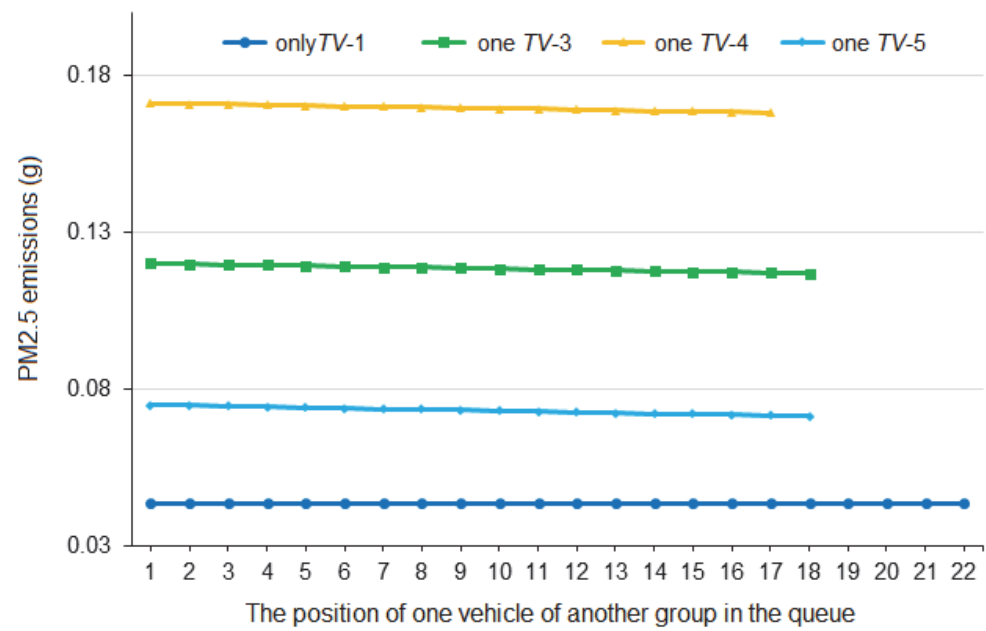


Figure 18. PM2.5 emissions if there is a vehicle of another group in the queue of passenger cars.

The expected decrease in total emissions from a full queue, as the ratio of emissions if a vehicle of another group is last in queue to emissions if a vehicle of another group is first in queue, is still rather insignificant. The emissions decrease for vehicles of various groups is:

- If there is one TV-3 in the queue—2.67%;
- If there is one TV-4 in the queue—1.76%;
- If there is one TV-5 in the queue—4.8%.

This insignificant change in total emissions is also explained by the small contribution of running exhaust emissions in relation to PM2.5 emissions during braking and acceleration. Figure 18 also demonstrates downward trends in the traffic capacity of the traffic flow if there is a vehicle of another group in a homogeneous queue of passenger cars.

6.3. PM2.5 Emissions If the Queue Contains Several Vehicles of One Group

It is expedient to consider a more complex traffic flow structure when a full queue of passenger cars contains several vehicles of other groups. In the first approach, let us consider situations when the queue contains several vehicles of only one of the groups: the third, fourth or fifth.

The general formula for calculating emissions from such a complex queue is based on formula (4), which determines the decrease in the intersection capacity. So, for a full queue of passenger cars containing several (N_i) vehicles of the i -th group, the emission calculation formula M_{ZZ1i} is as follows:

$$M_{ZZ1i} = N_i \cdot (M_{Zi} + M_{Li}) + N_i \cdot (M_{Z1} + M_{L1}), \tag{12}$$

where N_1 is the number of passenger cars that complete the queue, taking into account the coefficient k_i of reducing the vehicle from the i -th group to the first group, which is determined by the ratio: $N_1 = 22 - N_i \cdot (k_i - 1) - 2$; M_{Zi} and M_{Li} are emissions from one vehicle of the i -th group for the deceleration-acceleration phase and the running phase.

Figure 19 presents the graphical dependences of total PM2.5 emissions with an increase in the number of vehicles from another group in the full queue of passenger cars.

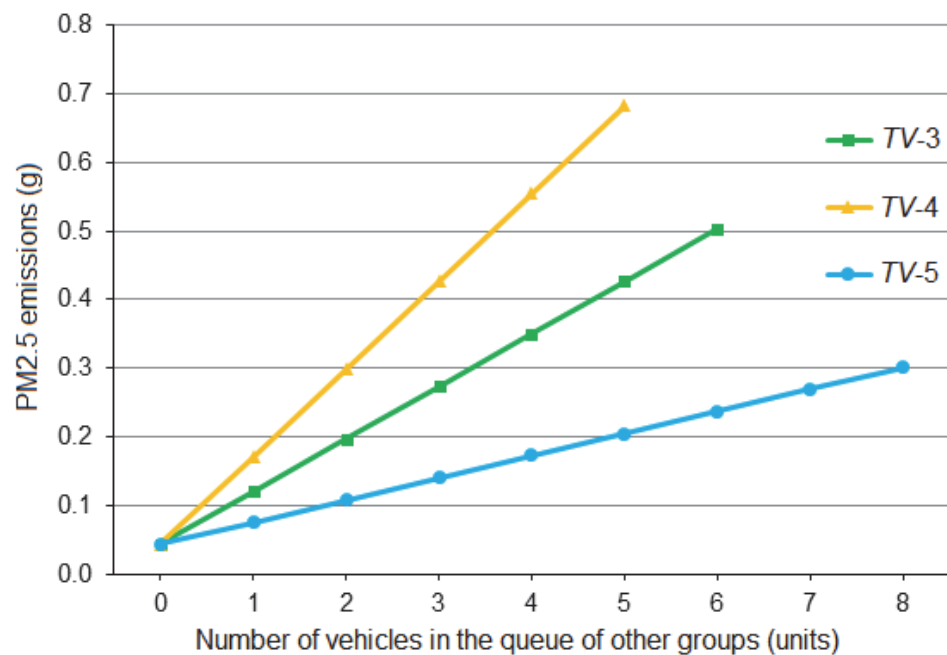


Figure 19. Total PM2.5 emissions if there are several vehicles of another group in the queue of passenger cars.

As follows from the analysis, only six TV-3 vehicles; five TV-4 vehicles, and eight TV-5 vehicles can join the full queue of 22 vehicles. This is determined by generally accepted replacement factors k_i .

6.4. PM2.5 Emissions If the Queue Contains Several Vehicles of Various Groups

In the second approach, let us consider the most general situation, when the queue consists of several vehicles from various groups: the third, fourth, or fifth.

Taking into account the unified speed profile for vehicles of the third and fourth groups, let us construct the distribution field of total PM2.5 emissions if the full queue of passenger cars contains the permissible number of vehicles of only the third and fifth groups.

The general formula for calculating emissions from such a combined queue is formed similar to formula (12), which simultaneously contains vehicles of the third and fifth groups. So, for the full queue of passenger cars containing N_3 TV-3 vehicles and N_5 vehicles of TV-5 group, the emission calculation formula M_{ZZ135} is:

$$M_{ZZ135} = N_3 \cdot (M_{Z3} + M_{L3}) + N_5 \cdot (M_{Z5} + M_{L5}) + N_1 \cdot (M_{Z1} + M_{L1}), \quad (13)$$

where N_1 is the number of passenger cars that complete the queue, taking into account the reduction factors k_3 and k_5 , which is determined by the ratio: $N_1 = 22 - N_3 \cdot (k_3 - 1) - N_5 \cdot (k_5 - 1) - 2$; M_{Zi} and M_{Li} are emissions from one vehicle of the i -th group for the deceleration-acceleration phase and the running phase.

Figure 20 presents a three-dimensional distribution field for total PM2.5 emissions in grams with an increase in the number of vehicles of the third and fifth groups in the full queue of passenger cars.

Here, the maximum possible combinations of the number of vehicles of the third and fifth groups are reflected in a horizontal projection.

To understand better the field of estimates for the emissions calculated by formula (13), Table 5 presents the ratios of PM2.5 emissions from a queue of an arbitrary composition to a full queue of 22 passenger cars taken as a unit.

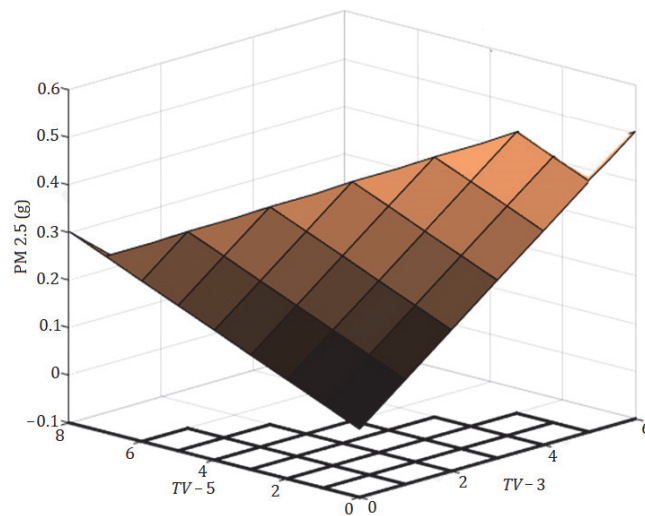


Figure 20. Distribution field for total PM2.5 emissions if the queue contains vehicles of two groups.

Table 5. Estimated increase in PM2.5 emissions with changes in the composition of the vehicle queue.

Assessment of the Increase PM2.5		Number of the TV-3 Group						
		0	1	2	3	4	5	6
Number of TV-5 group	0	1.00	2.76	4.53	6.30	8.07	9.84	11.60
	1	1.74	3.51	5.28	7.04	8.81	10.58	
	2	2.49	4.25	6.02	7.79	9.56	11.32	
	3	3.23	5.00	6.76	8.53	10.30		
	4	3.98	5.74	7.51	9.28			
	5	4.72	6.49	8.25				
	6	5.47	7.23					
	7	6.21						
8	6.95							

When vehicles from TV-3 and TV-5 are included in the full queue, the PM2.5 emissions are at most predicted to increase by 11.32 fold. The queue consists of five TV-3 vehicles and two TV-5 vehicles.

The restrictions on the possible combination of vehicles in a full queue crossing through the intersection area during one traffic light cycle are also clearly visible here.

7. Fuzzy Logic Method for Assessing Pollutant Emissions

Fuzzy logic methods [33,34,36] have become widespread in solving the problems of uncertainty and subjectivity typical of environmental monitoring. Full and highly accurate description and modeling of complex systems using mathematical tools are impossible, since input data are inaccurate or uncertain information and linguistic variables. The advantages of fuzzy logic include its flexibility and ease of understanding, as well as resistance to fuzzy data. Therefore, fuzzy logic methods in such complex processes as forecasting or modeling of environmental processes can cope with uncertainties in environmental data, have been successfully widely used and have provided reliable results.

The above approaches to estimating PM2.5 particulate matter emissions from traffic flows within a signal-controlled intersection do not take into account many random factors such as meteorological conditions, seasonality, and roadbed quality. Generally, it is expedient to approach estimating emissions as a fuzzy modeling problem based on the fuzzy set concept. E. Mamdani’s algorithm has gained practical use to avoid excessively large calculations.

To minimize the calculated load on the block of input variables, we chose only three levels for them. The mathematical expectation and standard deviation (sigma) or variance

are decisive for Gaussian random variables. Mathematical expectation for each term is determined by its expected middle, which is determined by the weight load of flows in terms of input variables. The width of the term is determined according to the “three-sigma” rule, based on the desire to overlap the possible flow range for the corresponding mathematical expectation. Expert assessments themselves are really taken from the practical experience of working with large amounts of information from both the software system and the reports of public institutions on laboratory measurements of pollutant emissions at urban intersections.

Let us consider the implementation of a predictive model based on the fuzzy logic method and the fuzzyTECH 8.77e software as the most general approach to estimating PM2.5 emissions in an intersection. The estimates of all variables are based on the calculated data from Table 2: the degree of increase in PM2.5 emissions due to the presence of vehicles of other groups in a queue of passenger cars is estimated V_{PM} ; independent input variables include the number of vehicles from group 1 TV_1 , group 3 TV_3 , and group 5— TV_5 . The block diagram of the constructed model is shown in Figure 21.

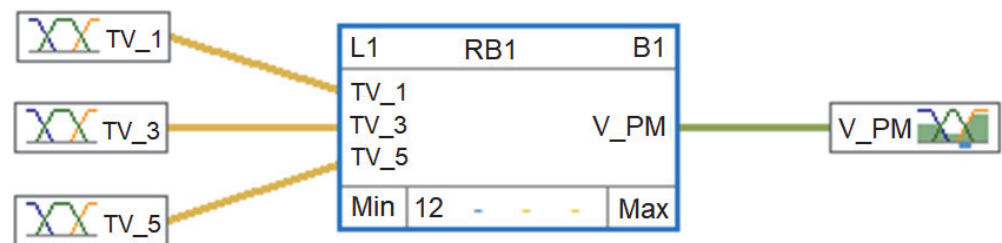


Figure 21. Block diagram of a predictive model based on the fuzzy logic method.

During fuzzification of variables, Gaussian membership functions were chosen as splines as they are most appropriate to state the problem stochastically. The parameters of the Gaussian terms were determined according to estimates taken from our practical work with surveillance camera data. Two terms are taken for the input variables TV_3 and TV_5 due to the small real range of their variations (up to 4 and up to 3, respectively); three terms with variations up to 20 are taken for TV_1 . Five terms are taken for the output variable V_{PM} , with variations up to 10 according to Table 2. The distribution of values over the terms of the variables TV_1 and V_{PM} is exemplified in Figure 22a,b, respectively.

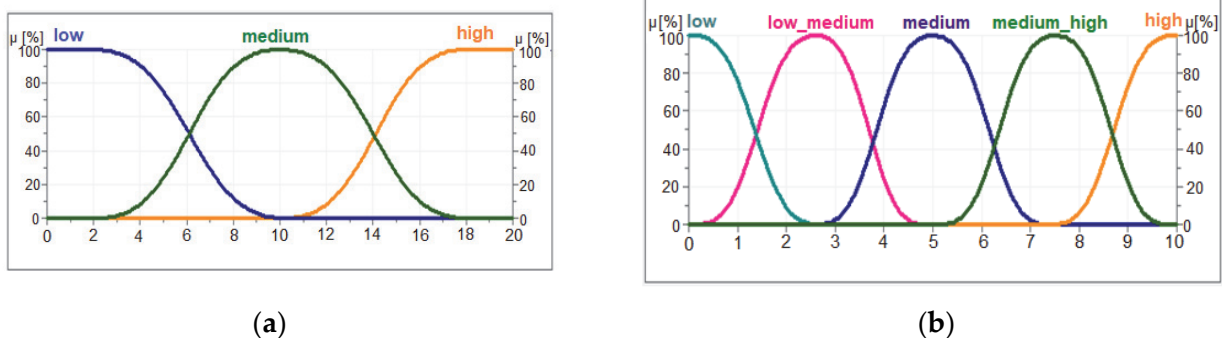


Figure 22. Distribution of the term values for the variables: (a) Output variable TV_1 ; (b) Output variable V_{PM} .

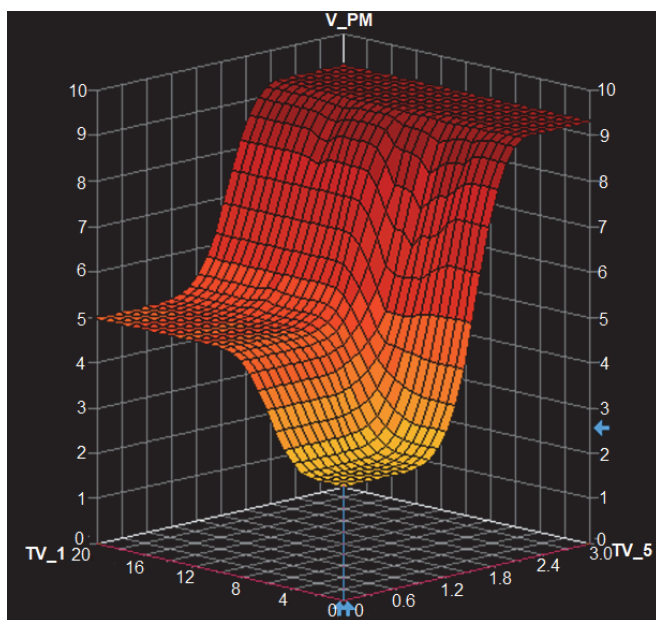
A fuzzy logic model for predicting V_{PM} values was defined by a table of its relationships with the input variables using the Spreadsheet rule editor block (Figure 23). Notably, anomalies related to inconsistency and consistency of the rules of relationships in the table are not considered at this stage. We plan to test fuzzy rules with a static and dynamic approach in our future detailed application of fuzzy logic methods.

	If	And	And	Then
B1	1	2	3	1
B1.G1	TS ₁	TS ₃	TS ₅	V _{PM}
B1.G1.R1	TS _{1.low}	TS _{3.low}	TS _{5.low}	V _{PM.low}
B1.G1.R2	TS _{1.low}	TS _{3.low}	TS _{5.high}	V _{PM.low_medium}
B1.G1.R3	TS _{1.low}	TS _{3.high}	TS _{5.low}	V _{PM.low_medium}
B1.G1.R4	TS _{1.low}	TS _{3.high}	TS _{5.high}	V _{PM.high}
B1.G1.R5	TS _{1.medium}	TS _{3.low}	TS _{5.low}	V _{PM.low}
B1.G1.R6	TS _{1.medium}	TS _{3.low}	TS _{5.high}	V _{PM.medium}
B1.G1.R7	TS _{1.medium}	TS _{3.high}	TS _{5.low}	V _{PM.medium}
B1.G1.R8	TS _{1.medium}	TS _{3.high}	TS _{5.high}	V _{PM.high}
B1.G1.R9	TS _{1.high}	TS _{3.low}	TS _{5.low}	V _{PM.low}
B1.G1.R10	TS _{1.high}	TS _{3.low}	TS _{5.high}	V _{PM.medium}
B1.G1.R11	TS _{1.high}	TS _{3.high}	TS _{5.low}	V _{PM.medium}
B1.G1.R12	TS _{1.high}	TS _{3.high}	TS _{5.high}	V _{PM.high}

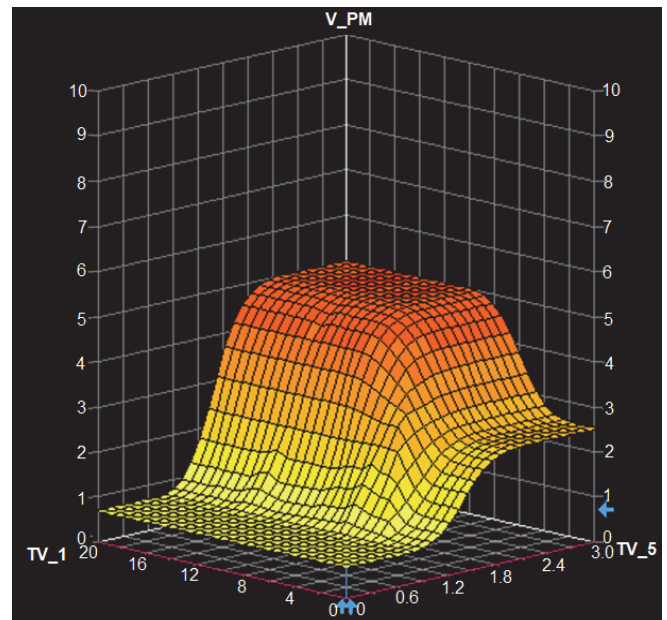
Figure 23. Table of rules for the relationship of model variables.

Experimental studies of the constructed model allow us to predict V_{PM} for the most realistic conditions (number of vehicles in the queue) and create a volumetric surfaces graph of the distribution field of the mutual influence of the variables.

We are mostly interested in PM_{2.5} emissions in the intersection depending on the number of vehicles from TV_1 and TV_5 , with two variations in the number of TV_3 vehicles in the queue. Figure 24 shows the distribution fields for the emissions forecast (variable V_{PM}) depending on TV_1 and TV_5 , with the maximum and minimum inclusion of TV_3 vehicles in the queue.



(a)



(b)

Figure 24. Forecasts of PM_{2.5} emissions depending on the queue structure: (a) Maximum for TV_3 ; (b) minimum for TV_3 .

The forecasting results using fuzzy sets of initial data is in good agreement with a priori expert estimates and can serve as a good foundation for making grounded decisions both on the formation of the traffic flow structure and signal-controlled intersection management.

To verify the suitability of the developed air quality monitoring model, we conducted validation testing: the comparison of theoretical calculations for fine particle matter concentrations PM2.5 with field measurements obtained through the integration of data from the software system used by the “Center for Environmental Monitoring”, including an advanced particulate measurement device called DustTrack 8533 [44]. These preliminary estimates revealed an average 18% deviation between measured values and modeled predictions, likely due to local sources of pollution from nearby industrial activities within the city (Figure 25). Examining the trend over time reveals how actual pollutant levels tend to peak later in the day than anticipated by the model, resulting in greater differences between observed and predicted concentrations towards the end of the workday.

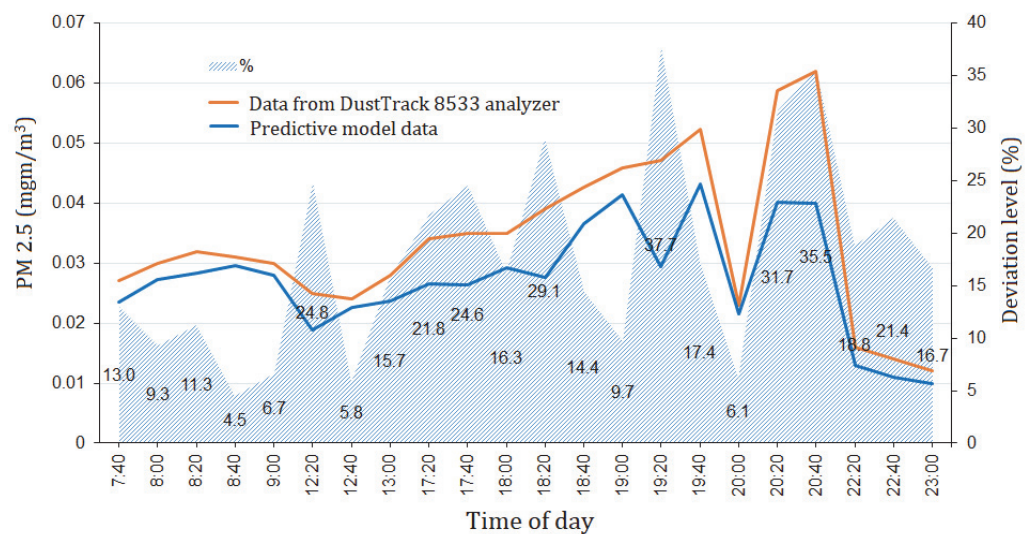


Figure 25. Comparison of the forecasted and measured PM2.5 emission concentrations.

8. Discussion

Intelligent vision based on neural network algorithms allowed us to generate an unlimited set of initial data on traffic within an intersection. Our analysis on the influence of variations in the traffic flow structure on the traffic capacity and changes in PM2.5 emissions are valid only for the chosen intersection. However, since we considered only the straight movement of vehicles and ignored the arrangement of left and right turns, the obtained results can be deemed fair for any signal-controlled intersection, especially since most of the results are presented in terms of their relation to a flow of passenger cars.

During the analysis, we obtained limit estimates of changes in the traffic capacity and pollutant emissions in the conditions of the maximum possible traffic flow. To this end, we preliminarily confirmed the generally accepted statistical estimate of the 2-s time interval between moving cars and obtained average statistical estimates of the acceleration of various types of vehicles when the green traffic light signal was turned on. For example, cars and trucks accelerate uniformly to a constant speed of 57 km/h and 48 km/h, respectively. The acceleration of buses to a cruising speed of 45 km/h is non-linear, but smooth to ensure the comfort of passengers. Notably, these estimates can be considered identical for the intersections of a similar structure in the entire urban transport network.

The main result of the analytical part is the limit estimates of the traffic capacity of the intersection and emissions of the most harmful pollutants—PM2.5 particulate matter. The analysis was based on a single methodology: the presence of one vehicle of another type in the queue of vehicles; the presence of several vehicles of a different type in the queue; the general 3D distribution field for an arbitrary traffic flow structure. So, if there is one vehicle of another group (TV-3, TV-4, or TV-5) in the queue of passenger cars, the traffic capacity

is reduced by an average of 20%, while the maximum number of vehicles of other groups crossing the intersection at the green traffic light signal is 6 vehicles of the *TV-3* group, or *TV-5* vehicles of the *TV-4* group, or 8 vehicles of the *TV-5* group.

When analyzing the amount of PM_{2.5}, we found that the presence of one vehicle of the third group in the queue of passenger cars leads to an increase in PM_{2.5} emissions by 2.7 fold in relation to the queue consisting only of passenger cars. If there is one vehicle of the *TV-4* group, emissions increase by 3.9 fold, and if there is one vehicle of the *TV-5* group—by 1.7 fold. Similarly, at the maximum number of vehicles of other groups crossing the intersection at the green traffic light signal: if there are 6 vehicles of the *TV-3* group, PM_{2.5} emissions increase by 11.6 fold; 5 vehicles of the *TV-4* group—by 14 fold, 8 vehicles of the *TV-5* group—by 7 fold in relation to the queue consisting only of passenger cars.

The interval between the theoretical estimates for the limit saturation traffic flow was presented using a probabilistic approach based on fuzzy logic methods. The obtained 3D distribution fields for PM_{2.5} emissions at arbitrary variations in the traffic flow confirm the revealed theoretical trends and provide for a better understanding of environmental problems in urban traffic flow management.

Our study estimated changes in traffic capacity and pollutant emissions with the maximum possible traffic flow and the absence of congestion. That is, the obtained estimates are limited to a signal-controlled intersection. Real situations will be characterized by lower values of the obtained estimates if the traffic flow is less intensive than the saturation flow and larger values in case of a traffic jam within the intersection.

For complete transferability and scalability of the obtained results to any signal-controlled intersection, we plan to further develop a common model of an intersection when vehicles are moving in all directions, taking into account right and left turns, based on the limiting values of saturation flows (but without traffic jams).

9. Conclusions

This study presents a new approach to assessing the urban traffic flow and the atmospheric dispersion of pollutants using machine learning methods. The use of a neural network to extract information related to specific vehicle classes and fuzzy logic methods with Gaussian spline relevance functions gives a basis for understanding the relationship between the traffic flow/concentration and the vehicle type/classification, which provides for a better understanding of the best management of road space distribution and emissions under different circumstances. Based on the algometric method, we obtained theoretical dependences of the reduction in the traffic capacity and harmful emissions depending on the situational structure of the traffic jam and the operating mode of the traffic light. As a result of data processing, we revealed that the heterogeneous composition of the queue of vehicles of different classes reduces the traffic capacity of the traffic lane at a signal-controlled intersection in varying degrees. So, for example, if there are three vehicles of the fifth group (buses) in the queue of passenger cars, the traffic capacity is reduced to 70%. The maximum reduction in the traffic capacity with an arbitrary structure of the traffic flow reaches 32% relative to the queue of passenger cars. The most notable finding is the exponential growth in emissions from buses or more than three buses in the queue of passenger cars, which increased emissions by 14 fold. The proposed method provides new insights into traffic management optimization and air pollution mitigation. Our study suggests possible further improving ambient air quality in densely populated urban centers facing increasing transport challenges in the conditions of a limited budget. These findings are essential for traffic planning and environmental policy development. Our further work will focus on refining the models and expanding their capabilities to build an optimal structure for the vehicle queue at the entrance to intersections, in order to reduce the negative environmental impact.

Author Contributions: Conceptualization, V.S. and A.G.; methodology, I.S.; software, I.S.; validation, M.B. and A.G.; investigation, A.G.; resources, I.S.; writing—original draft preparation, V.S.; writing—review and editing, A.G.; visualization, M.B.; supervision, V.S. All authors have read and agreed to the published version of the manuscript.

Funding: This research received no external funding.

Data Availability Statement: Not applicable.

Conflicts of Interest: The authors declare no conflict of interest.

References

1. EEA. Air Quality in Europe 2021. Available online: <https://www.eea.europa.eu//publications/air-quality-in-europe-2022> (accessed on 3 March 2023).
2. Mulholland, E.; Miller, J.; Bernard, Y.; Lee, K.; Rodríguez, F. The role of NOx emission reductions in Euro 7/VII vehicle emission standards to reduce adverse health impacts in the EU27 through 2050. *Transp. Eng.* **2022**, *9*, 100133. [CrossRef]
3. Kulakarni, R.; Cheपुरi, A.; Arkatkar, S.; Joshi, G.J. Estimation of saturation flow at signalized intersections under heterogeneous traffic conditions. In *Transportation Research*; Mathew, T., Joshi, G., Velaga, N., Arkatkar, S., Eds.; Springer: Singapore, 2020; Volume 45. [CrossRef]
4. Aoyama, E.; Yoshioka, K.; Shimokawa, S.; Morita, H. Estimating saturation flow rates at signalized intersections in Japan. *Asian Transp. Stud.* **2020**, *6*, 100015. [CrossRef]
5. Wu, N.; Giuliani, S. Capacity and Delay Estimation at Signalized Intersections Under Unsaturated Flow Condition Based on Cycle Overflow Probability. In Proceedings of the International Symposium on Enhancing Highway Performance, Berlin, Germany, 14–16 June 2016; Volume 15, pp. 63–74. [CrossRef]
6. Jin, X.; Zhang, Y.; Wang, F.; Li, L.; Yao, D.; Su, Y.; Wei, Z. Departure headways at signalized intersections: A log-normal distribution model approach. *Transp. Res. Part C Emerg. Technol.* **2009**, *17*, 318–327. [CrossRef]
7. Sun, L.; Tao, J.; Li, C.; Tong, Z.; Wang, S. Microscopic simulation and optimization of signal timing based on multi-agent: A case study of the intersection in Tianjin. *KSCE J. Civ. Eng.* **2018**, *22*, 3373–3382. [CrossRef]
8. Ding, S.Z.; Chen, X.M.; Yu, L. Markov chain-based platoon recognition model in mixed traffic with human-driven and connected and autonomous vehicles. *J. Cent. South Univ.* **2022**, *29*, 1521–1536. [CrossRef]
9. Eom, M.; Kim, B.I. The traffic signal control problem for intersections: A review. *Eur. Transp. Res. Rev.* **2020**, *12*, 50. [CrossRef]
10. HCM 2010: *Highway Capacity Manual*; Transportation Research Board: Washington, DC, USA, 2010.
11. Mohan, M.; Chandra, S. Three methods of PCU estimation at unsignalized intersections. *Transp. Lett.* **2018**, *10*, 68–74. [CrossRef]
12. Mandal, A.; Sadhukhan, P.; Gaji, F.; Sharma, P. Measuring Real-Time Road Traffic Queue Length: A Reliable Approach Using Ultrasonic Sensor. In Proceedings of the 2nd International Conference on Communication, Devices and Computing, Haldia, India, 14–15 March 2019. [CrossRef]
13. Pandian, S.; Gokhale, S.; Ghoshal, A.K. Evaluating effects of traffic and vehicle characteristics on vehicular emissions near traffic intersections. *Transp. Res. Part D Transp. Environ.* **2009**, *14*, 180–196. [CrossRef]
14. Dhamaniya, A.; Bari, C.S.; Patkar, M. Capacity analysis of urban arterial midblock sections under mixed traffic conditions. *Int. J. ITS Res.* **2022**, *20*, 409–421. [CrossRef]
15. Singh, S.; Santhakumar, S.M. Platoon-based impact assessment of heavy-duty vehicles on traffic stream characteristics of highway lanes under mixed traffic environment. *Int. J. Intell. Transp. Syst. Res.* **2022**, *20*, 29–45. [CrossRef]
16. Parmar, D.; Gore, N.; Rathva, D.; Dave, S.; Jain, M. Modelling Queuing of Vehicles at Signalized Intersection. In Proceedings of the 4th Conference of Transportation Research Group of India, Mumbai, India, 17–20 December 2017. [CrossRef]
17. Zhu, F.; Lo, H.K.; Lin, H.-Z. Delay and emissions modelling for signalised intersections. *Transp. B Transp. Dyn.* **2013**, *1*, 111–135. [CrossRef]
18. Goel, A.; Kumar, P. A review of fundamental drivers governing the emissions, dispersion and exposure to vehicle-emitted nanoparticles at signalised traffic intersections. *Atmos. Environ.* **2014**, *97*, 316–331. [CrossRef]
19. Yassin, M.F.; Kellnerová, R.; Jaňour, Z. Impact of street intersections on air quality in an urban environment. *Atmos. Environ.* **2008**, *42*, 4948–4963. [CrossRef]
20. Woodward, H.; Stettler, M.; Pavlidis, D.; Aristodemou, E.; ApSimon, H.; Pain, C. A large eddy simulation of the dispersion of traffic emissions by moving vehicles at an intersection. *Atmos. Environ.* **2019**, *215*, 116891. [CrossRef]
21. Liu, H.; Zhang, Y.; Zhang, K. Evaluating impacts of intelligent transit priority on intersection energy and emissions. *Transp. Res. Part D Transp. Environ.* **2020**, *86*, 102416. [CrossRef]
22. Jaikumar, R.; Shiva Nagendra, S.M.; Sivanandan, R. Modal analysis of real-time, real world vehicular exhaust emissions under heterogeneous traffic conditions. *Transp. Res. Part D Transp. Environ.* **2017**, *54*, 397–409. [CrossRef]
23. Ritner, M.; Westerlund, K.K.; Cooper, C.D.; Claggett, M. Accounting for acceleration and deceleration emissions in intersection dispersion modeling using MOVES and CAL3QHC. *J. Air Waste Manag. Assoc.* **2013**, *63*, 724–736. [CrossRef]
24. Wang, C.; Ye, Z.; Bi, H. Exploring the influence of contributing factors and impact degree on bus emissions in real-world conditions. *Env. Sci. Pollut. Res.* **2021**, *28*, 36092–36101. [CrossRef]

25. Song, L.; Fan, W. Intersection capacity adjustments considering different market penetration rates of connected and automated vehicles. *Transp. Plan. Technol.* **2023**, *46*, 286–303. [[CrossRef](#)]
26. Tu, R.; Alfaseeh, L.; Djavadian, S.; Farooq, B.; Hatzopoulou, M. Quantifying the impacts of dynamic control in connected and automated vehicles on greenhouse gas emissions and urban NO₂ concentrations. *Transp. Res. Part D Transp. Environ.* **2019**, *73*, 142–151. [[CrossRef](#)]
27. Han, S.-C.; Wang, G.-Z.; Zhou, G.-B. Air pollution, EGFR mutation, and cancer initiation. *Cell Rep. Med.* **2023**, *4*, 101046. [[CrossRef](#)] [[PubMed](#)]
28. Tomson, M.; Kumar, P.; Kalaiarasan, G.; Zavala-Reyes, J.; Chiapasco, M.; Sephton, M.; Young, G.; Porter, A. Pollutant concentrations and exposure variability in four urban microenvironments of London. *Atmos. Environ.* **2023**, *298*, 119624. [[CrossRef](#)]
29. Kamboures, M.A.; Rieger, P.L.; Zhang, S.; Sardar, S.B.; Chang, M.-C.O.; Huang, S.-M.; Ayala, A. Evaluation of a method for measuring vehicular PM with a composite filter and a real-time BC instrument. *Atmos. Environ.* **2015**, *123*, 63–71. [[CrossRef](#)]
30. Benson, P.E. A review of the development and application of the CALINE3 and 4 models. *Atmos. Environ. Part B Urban Atmos.* **1992**, *26*, 379–390. [[CrossRef](#)]
31. Ntziachristos, L.; Gkatzoflias, D.; Kouridis, C.; Samaras, Z. COPERT: A European Road Transport Emission Inventory Model. In Proceedings of the 4th International ICSC Symposium, Thessaloniki, Greece, 28–29 May 2009. [[CrossRef](#)]
32. Rodler, S.J.; Sturm, P.; Rexeis, M. Emission factors for heavy-duty vehicles and validation by tunnel measurements. *Atmos. Environ.* **2003**, *37*, 5237–5245. [[CrossRef](#)]
33. Lyu, P.; Wang, P.; Liu, Y.; Wang, Y. Review of the studies on emission evaluation approaches for operating vehicles. *J. Traf Transp. Eng.* **2021**, *8*, 493–509. [[CrossRef](#)]
34. Carbajal-Hernández, J.J.; Sánchez-Fernández, L.P.; Carrasco-Ochoa, J.A.; Martínez-Trinidad, J.F. Assessment and prediction of air quality using fuzzy logic and autoregressive models. *Atmos. Environ.* **2012**, *60*, 37–50. [[CrossRef](#)]
35. Prasad, K.; Gorai, A.K.; Goyal, P. Development of ANFIS models for air quality forecasting and input optimization for reducing the computational cost and time. *Atmos. Environ.* **2016**, *128*, 246–262. [[CrossRef](#)]
36. Yang, H.; Zhu, Z.; Li, C.; Li, R. A novel combined forecasting system for air pollutants concentration based on fuzzy theory and optimization of aggregation weight. *Appl. Soft Comput.* **2020**, *87*, 105972. [[CrossRef](#)]
37. Video Surveillance of Intersections and Streets in Chelyabinsk in Real Time. Available online: <https://cams.is74.ru/live> (accessed on 12 February 2023).
38. Bochkovskiy, A.; Wang, C.Y.; Liao, H.Y.M. Yolov4: Optimal Speed and Accuracy of Object Detection. 23 April 2020. Available online: <https://arxiv.org/pdf/2004.10934.pdf> (accessed on 2 May 2022).
39. Bewley, A.; Ge, Z.; Ott, L.; Ramos, F.; Upcroft, B. Simple Online and Realtime Tracking. In Proceedings of the IEEE international conference on image processing, Phoenix, AZ, USA, 25–28 September 2016. [[CrossRef](#)]
40. Khazukov, K.; Shepelev, V.; Karpeta, T.; Shabiev, S.; Slobodin, I.; Charbadze, I.; Alferova, I. Real-time monitoring of traffic parameters. *J. Big Data* **2020**, *7*, 84. [[CrossRef](#)]
41. Order of the Ministry of Natural Resources and Ecology of the Russian Federation No. 804 Dated 27 November 2019 “On Approval of the Methodology for Determining Emissions of Pollutants into the Atmospheric air from Mobile Sources for Conducting Summary Calculations of Atmospheric Air Pollution”. Available online: <https://www.garant.ru/products/ipo/prime/doc/73240708/> (accessed on 7 November 2022).
42. Order of the Ministry of Natural Resources and Ecology of the Russian Federation No 273 Dated 6 June 2017 “On Approval of Methods for Calculating the Dispersion of Emissions of Harmful (Polluting) Substances in the Atmospheric Air”. Available online: <https://docs.cntd.ru/document/456074826> (accessed on 7 November 2022).
43. Shepelev, V.; Glushkov, A.; Slobodin, I.; Cherkassov, Y. Measuring and modelling the concentration of vehicle-related PM_{2.5} and PM₁₀ emissions based on neural networks. *Mathematics* **2023**, *11*, 1144. [[CrossRef](#)]
44. DustTrak™ DRX Aerosol Monitor 8533. Available online: <https://tsi.com/products/aerosol-and-dust-monitors/aerosol-and-dust-monitors/dusttrak%E2%84%A2-drx-aerosol-monitor-8533/> (accessed on 9 May 2023).

Disclaimer/Publisher’s Note: The statements, opinions and data contained in all publications are solely those of the individual author(s) and contributor(s) and not of MDPI and/or the editor(s). MDPI and/or the editor(s) disclaim responsibility for any injury to people or property resulting from any ideas, methods, instructions or products referred to in the content.